Theses and Dissertations | 1. Thesis and Dissertation Collection, all items

1984

# Simulation of the coupled atmospheric and oceanic boundary layer model during MILDEX.

Swaykos, Joseph W.

http://hdl.handle.net/10945/19555

# NAVAL POSTGRADUATE SCHOOL
## Monterey, California
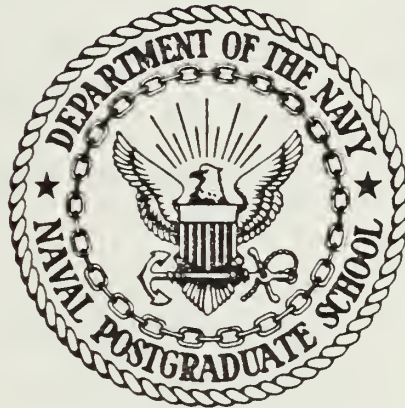
# THESIS

SIMULATION OF THE COUPLED ATMOSPHERIC AND
OCEANIC BOUNDARY LAYER MODEL DURING MILDEX

by

Joseph W. Swaykos

December 1984

Thesis Advisor: R.W. Garwood

| REPORT DOCUMENTATION PAGE | | READ INSTRUCTIONS<br>BEFORE COMPLETING FORM |
|---|---|---|
| 1. REPORT NUMBER | 2. GOVT ACCESSION NO. | 3. RECIPIENT'S CATALOG NUMBER |
| 4. TITLE *(and Subtitle)*<br><br>Simulation of the Coupled Atmospheric and Oceanic Boundary Layer Model During MILDEX | | 5. TYPE OF REPORT & PERIOD COVERED<br><br>Master's Thesis<br>December 1984 |
| | | 6. PERFORMING ORG. REPORT NUMBER |
| 7. AUTHOR(s)<br><br>Joseph W. Swaykos | | 8. CONTRACT OR GRANT NUMBER(s) |
| 9. PERFORMING ORGANIZATION NAME AND ADDRESS<br><br>Naval Postgraduate School<br>Monterey, CA 93943 | | 10. PROGRAM ELEMENT, PROJECT, TASK AREA & WORK UNIT NUMBERS |
| 11. CONTROLLING OFFICE NAME AND ADDRESS<br><br>Naval Postgraduate School<br>Monterey, CA 93943 | | 12. REPORT DATE<br><br>December 1984 |
| | | 13. NUMBER OF PAGES<br>67 |
| 14. MONITORING AGENCY NAME & ADDRESS *(if different from Controlling Office)* | | 15. SECURITY CLASS. *(of this report)* |
| | | 15a. DECLASSIFICATION/DOWNGRADING SCHEDULE |

16. DISTRIBUTION STATEMENT *(of this Report)*

Approved for public release; distribution is unlimited

17. DISTRIBUTION STATEMENT *(of the abstract entered in Block 20, if different from Report)*

18. SUPPLEMENTARY NOTES

19. KEY WORDS *(Continue on reverse side if necessary and identify by block number)*

Coupled Boundary Layer Model        Air-Sea Interaction
Atmospheric Boundary Layer          Oceanic Boundary Layer
MILDEX

20. ABSTRACT *(Continue on reverse side if necessary and identify by block number)*

A coupled, oceanic-atmospheric boundary layer model which provides single-station prediction capability is evaluated relative to boundary layer observations. The model is initialized and verified using data obtained during the 1983 Mixed Layer Dynamics Experiment (MILDEX). Model prediction of inversion height, lifting condensation level, air and sea temperatures, specific humidity and mixed layer depth are

DD ₁ FORM ₇₃ 1473    EDITION OF 1 NOV 65 IS OBSOLETE
S N 0102-LF-014-6601

compared with observations.   A significant model shortcoming is the over-prediction of cloud thickness.   Consequently, shortwave radiation at the ocean surface is too low and the predicted ocean mixed layer depths are not realistic.   Oceanic predictions resulting from independent specification of surface radiation more closely resembled observed oceanic variations.   Atmospheric boundary layer model reformulation is required to alleviate the cloud thickness/shortwave radiation problem.

Simulation of the
Coupled Atmospheric and Oceanic Boundary Layer Model
During MILDEX

by

Joseph W. Swaykos
Lieutenant Commander, U.S. Navy
B.S., United States Naval Academy, 1976
M.S., University of Southern California, 1982


Submitted in partial fulfillment of the
requirements for the degree of

MASTER OF SCIENCE IN METEOROLOGY AND OCEANOGRAPHY

from the

NAVAL POSTGRADUATE SCHOOL
December 1984

## ABSTRACT

A coupled, oceanic-atmospheric boundary layer model
which provides single-station prediction capability is eval-
uated relative to boundary layer observations. The model is
initialized and verified using data obtained during the 1983
Mixed Layer Dynamics Experiment (MILDEX). Model prediction
of inversion height, lifting condensation level, air and sea
temperatures, specific humidity and mixed layer depth are
compared with observations. A significant model shortcoming
is the over-prediction of cloud thickness. Consequently,
shortwave radiation at the ocean surface is too low and the
predicted ocean mixed layer depths are not realistic.
Oceanic predictions resulting from independent specification
of surface radiation more closely resembled observed oceanic
variations. Atmospheric boundary layer model reformulation
is required to alleviate the cloud thickness/shortwave radi-
ation problem.

# ACKNOWLEDGEMENTS

## TABLE OF CONTENTS

# LIST OF TABLES

.

7

## LIST OF FIGURES

9

# I. INTRODUCTION

All aspects of naval operations are affected by the adjacent ocean/atmosphere environment. The performance of weapons systems operating on the principles of electro-optical (EO) and electromagnetic (EM) physics are dependent upon the existing atmospheric conditions in the marine atmospheric boundary layer (MABL). Those systems whose operation is governed by water borne acoustic paths are dependent upon the environmental conditions in the ocean boundary layer. Aside from the exceptionally severe weather phenomena so commonly associated with environmental dynamics, the complex weapons systems in use throughout the fleet are affected by routine environmental conditions and subtle changes therein as well as by the renowned extremes.

Atmospheric dynamics will alter the vertical profiles of temperature, humidity and pressure which are the variables affecting the refractivity of the atmosphere. The vertical gradient of refractivity is the critical factor in the presence of phenomena such as ducting, subrefraction, super-refraction, frequency dependencies and their impact upon the performance of electro-optical and electromagnetic systems.

Oceanic dynamics manifest as vertical variations in temperature, pressure and salinity affect the sound speed profile. As the most critical factor in determining the propagation of acoustic energy, variations in the sound speed profile as a function of depth will result in phenomena such as surface ducting and convergence zones and will determine cutoff frequencies and optimal source/ receiver geometries.

Atmospheric and oceanic boundary layer processes are highly interdependent. The ability to predict their inter-action is clearly essential to the tactical commander.

10

The model evaluated consists of a one dimensional atmospheric model (Davidson et al., 1984) and a one dimensional oceanic boundary layer model (Garwood, 1977). The models were coupled (O'Laughlin, 1982) and demonstrated to realistically simulate boundary layer dynamics (Hervey, 1983). The goal of this study is to assess the ability of a coupled ocean-atmosphere boundary layer model to accurately make such predictions by conducting a boundary layer simulation using oceanic and atmospheric data obtained during the 1983 Mixed Layer Dynamics Experiment (MILDEX).

## II. BACKGROUND

### A. MOTIVATION

The evolution of the NPS coupled atmospheric and oceanic boundary layer model has reached the developmental stage of being used to predict atmospheric and oceanic dynamics using actual data sets for initialization and comparison with model output. Prior efforts along this model development path include an examination of the coupled model's ability to forecast using real data for initialization and comparison of results in order to determine the adequacy of the coupling (O'Laughlin, 1982). This study concluded that the coupled model did indeed yield fairly accurate results; however, the data sets employed (CEWCOM 1976 and CEWCOM 1978) were inadequate. The inadequacy was a result of the frequent transit of the data gathering vessel, RV ACANIA over significant distances through inhomogeneous water masses.

A follow-on study examined the adequacy of the coupled boundary layer model relative to the performance of the uncoupled atmospheric and oceanic models. The results indicated that the benefits of coupling to the MABL were minor; however, the predictive capability of the OBL was greatly enhanced (Hervey, 1983).

Both studies recommended evaluation with data sets where effects of advection and vessel movement are minimized. Such a data set was obtained during the 1983 Mixed Layer Dynamics Experiment (MILDEX) (Geernaert et al., 1984), conducted from October 24 through November 10, 1983. Data were obtained 3 to 5 November, 1983 in the vicinity of 34 N and 126 W by RV ACANIA (Fig. 2.1). Meteorological data

12
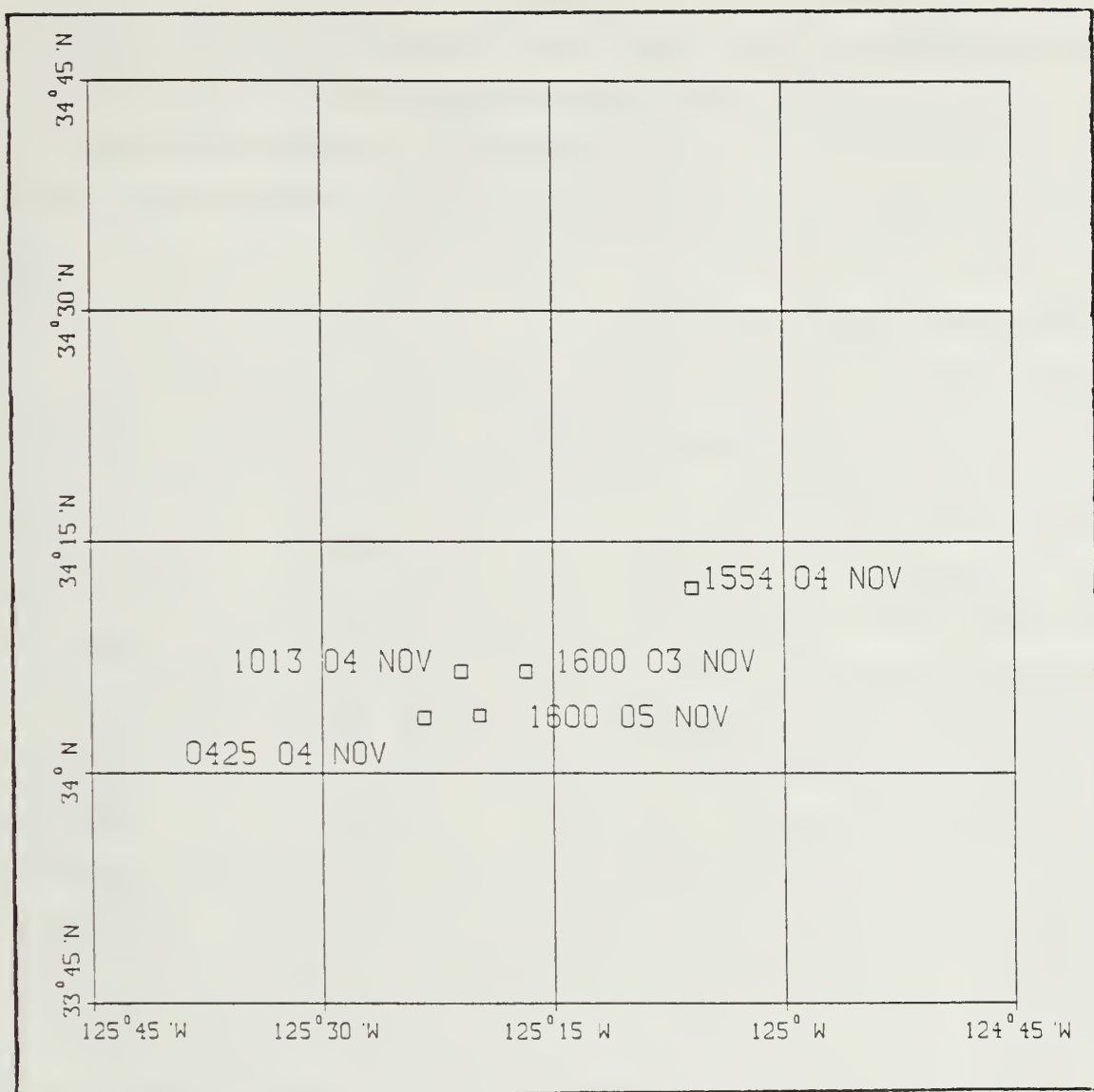
Figure 2.1    Positions of RV ACANIA: 03-05 Nov 1983

consisted of atmospheric pressure, windspeed, temperature,
humidity and radiation in the atmospheric surface layer.
Profiles of atmospheric wind speed and direction, tempera-
ture and humidity using a navaid radiosonde system were also
obtained.    Additionally, observations of sea state and
cloudiness were recorded hourly.

Oceanographic data were obtained with a Neil Brown Instrument System (NBIS) CTD. The device recorded values of temperature, conductivity, depth and dissolved oxygen. Two other research vessels, WACOMA and FLIP acquired data in the vicinity of ACANIA. FLIP was within 2 kilometers of the ACANIA from October 26 through November 9.

## B. BOUNDARY LAYER CHARACTERISTICS

The Marine Atmospheric Boundary Layer (MABL) extends from the air-sea interface through a capping inversion typically 100 to 1000m high. The Oceanic Boundary Layer (OBL) extends from the interface to the thermocline, 2 to 50m deep. The MABL is comprised of a cool, moist, turbulent well mixed layer (relative to the upper atmosphere) in which equivalent potential temperature and specific humidity are basically constant with height. At the inversion level a significant change (jump) in the vertical profiles of these variables occurs. The air above the inversion is warmer than that of the mixed layer and is characterized by a lapse rate of increasing temperature as a function of height. Similarly, the air of the free atmosphere is drier than that of the MABL with the moisture content decreasing as a function of height.

The value of the well mixed quantities change over time due to the turbulent fluxes of heat and moisture at the air-sea interface and at the inversion. Turbulent kinetic energy provides the necessary forcing of these processes. The turbulent kinetic energy budget provides the foundation upon which most of the modelling is based. The well mixed nature of the variables in the MABL and OBL imply that heat and moisture are conserved during the mixing process and that the variation with height of the vertical turbulent fluxes of momentum, humidity and heat is linear. Assuming

14

advection is negligible, these properties permit the modeling of the variation of the variables based solely upon surface and inversion layer height fluxes.

Turbulence at the inversion causes the entrainment of warm, dry air into the MABL and growth of the layer, large (synoptic) scale atmospheric forcing contributes to subsidence. The time rate of change of the height of the MABL is a result of these effects.

An important atmospheric feature is the presence of clouds. If the lifting condensation level (LCL) is lower than the height of the inversion, clouds will be present. A stratus layer in the MABL will vary the amount of solar, shortwave and return long wave radiation in the boundary layer. Such variations will greatly affect the dynamics of the MABL and OBL (Hervey, 1983).

The Oceanic Boundary Layer (OBL) is a turbulent region of the upper ocean bounded by a dynamically stable water mass at its base and by the air-sea interface above. The layer is characterized by constant velocity and density profiles arising from the high degree of turbulence within the layer and a relatively slight amount of turbulence in the underlying stable watermass. Momentum and buoyancy fluxes through the surface provide the energy which results in the boundary layer turbulence.

Density is a function of temperature and salinity, both of which are assumed to be homogeneous in the boundary layer. Since the model will forecast for relatively short periods of time (less than 72 hours), the effects of salinity are assumed to be negligible (Miller, 1976). As in the case of the MABL, the vertical homogeneity of the OBL allows for the modelling of dynamic processes through the use of only the surface and entrainment fluxes. The turbulent kinetic energy budget again serves as the foundation for modeling.

15

## C.   MIXED ATMOSPHERIC BOUNDARY LAYER MODEL (MABL)

The atmospheric variables required as input are short-wave radiation, which depends on Julian date, time of day and latitude, inversion height, mixed layer and jump values for equivalent potential temperature and specific humidity. Also the above layer lapse rates for specific humidity and potential temperature, subsidence rate, wind speed and direction within the mixed layer and sea surface temperature are required.   In the uncoupled model sea surface temperature is constant. However, the coupled model uses the variations in sea surface temperature as predicted by the OBL model as an input.

Three methods are available for the computation of subsidence (large scale vertical velocity). The methods are the kinematic, the adiabatic and the integration of the moisture budget equation (Q method). The Q method is the most accurate approach given single station data, according to Gleason (1982). It was used for subsidence calculation for this study.

The MABL predicts the evolution of the LCL, inversion height, mixed layer values of equivalent potential temperature and specific humidity, their respective jump values, entrainment rate, short and long wave radiation, friction velocity (U*), and the scaling parameters for temperature and humidity (T* and Q*) for a prescribed period. The model uses a 30 minute time step. The computational steps are depicted in Fig. 2.2.

The time evolution of the conservative variables are predicted using integrated (with respect to height) rate equations (Tennekes and Dreidonks, 1981). These equations are:

16
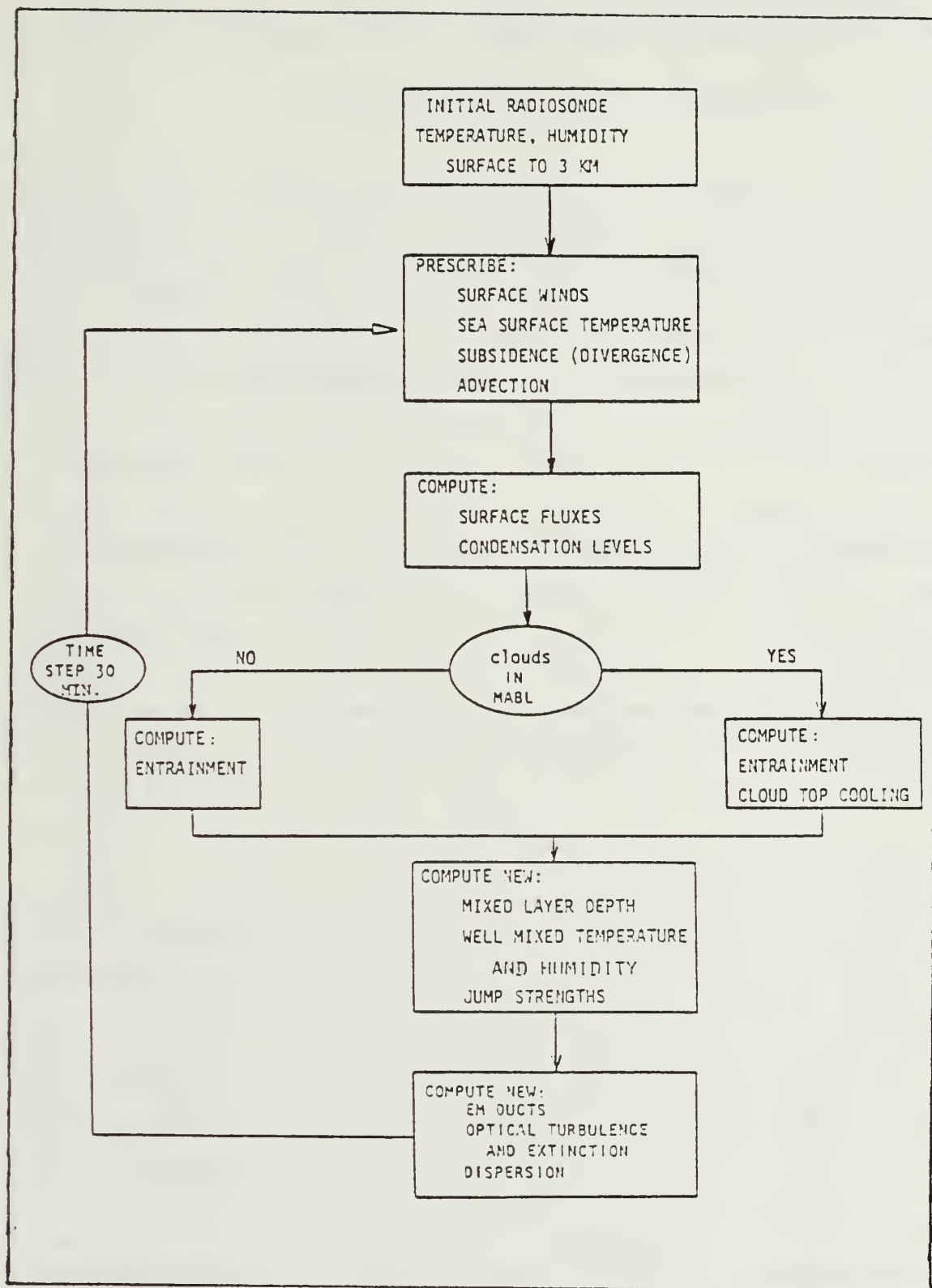
Figure 2.2    MABL Schematic

17

$$h(Dx/Dt) = (w'x')_o - (w'x')_h + source \qquad (2.1)$$

$$h(D\Delta x/Dt) = h\Gamma_x(\partial h/\partial t) - (w'x')_o + (w'x')_h - source \qquad (2.2)$$

where the subscripts zero and h refer to surface and inversion height values, respectively. Gamma ($\Gamma$) is the lapse rate above the inversion height and the source term is equal to $-(F_{nh} - F_{no})/\rho Cp$ for $X = \Theta$ and equal to zero for $X=q$. The subscripts h and zero refer to inversion height and surface, respectively, Fn is the net radiative flux. The quantity $(\partial h/\partial t)$ is the difference between the time rate of change of the inversion height $(dh/dt)$ and subsidence rate.

The system of equations is closed through the use of Stage and Businger's (1981) entrainment rate parameterization. This is also used in the determination of the temporal evolution of the inversion height. To obtain the entrainment rate, Stage and Businger made a closure assumption that the dissipation rate of turbulent kinetic energy is a fraction (1-A) of the production rate, P:

$$D = (1-A)P \qquad (2.3)$$

The quantity 'A' in essence is the critical flux Richardson number (Ricr) which separates turbulent from nonturbulent boundary layers. It has been determined through the modeling of dry convective layers that A=0.2. This value is in close agreement to that calculated by Businger (1973) and lies in the middle of the range of critical flux Richardson numbers, 0.15 to 0.25, which were determined by Arya (1972). Earlier modeling efforts indicated that only 1 to 4 percent of the TKE produced in the boundary layer was used for entrainment. The 0.2 factor however indicates that 20 percent of the TKE is thus utilized.

18

Bulk aerodynamic formulas are used in the determination of the surface fluxes of momentum, heat, and moisture:

$$U* = Cd^{1/2} U \tag{2.4}$$

$$T* = C_\theta^{1/2} (\theta - \theta_0) \tag{2.5}$$

$$q* = C_\theta^{1/2} (q - q_0) \tag{2.6}$$

The fluxes are represented by:

$$\overline{(u'w')} = U*^2 \tag{2.7}$$

$$\overline{(-T'w')} = U* T* \tag{2.8}$$

$$\overline{(-q'w')} = U* q* \tag{2.9}$$

Cd and Cθ are the stability dependent drag and exchange coefficients. The zero subscript refers to surface values, overbars represent average quantities and primes (') represent fluctuations from mean values.

Long and shortwave radiation fluxes are calculated independently. Modeling of these quantities is extremely difficult. Effects of absorbing aerosols and gases, and of the distribution of cloud droplet size, are nearly impossible to predict. Long wave radiation modeling is based upon empirical relations between the average cloud liquid water content and cloud emissivity. Cloud top net long wave radiative flux L is determined from the Stefan-Boltzman law and cloud top temperature:

$$L_{nh} = \epsilon_c \sigma (Th^4 - T_{sky}^4) \tag{2.10}$$

19

The parameter $\sigma$ is Stefan's constant and the parameter $\epsilon_c$ is determined by:

$$\epsilon_c = 1 - \exp(-aW) \qquad (2.11)$$

where $\epsilon_c$ is the cloud emissivity, $W$ is the cloud liquid water content, and 'a' is a constant equal to $.158\ m^2g^{-1}$ (Slingo, et al., 1982). Cloud base long wave radiative flux is represented by:

$$L_{nc} = \epsilon_c (Ts^4 - Tc^4) \qquad (2.12)$$

where Ts is the sea surface temperature and Tc is the cloud base temperature. Radiative flux divergence in the air between the sea surface and cloud base is neglected so that $L_{nc} = L_{ns}$. Therefore, the net long wave flux at the surface is given by:

$$F(long) = \sigma (Ts^4 - \epsilon_c \overline{T}^4 - (1 - \epsilon_c) T_{sky}^4) \qquad (2.13)$$

where $\overline{T}$ is the average cloud temperature.

For the cloud free condition, the net long wave flux is calculated at z=h and z=0 by integrating the flux emissivity profile as developed by Fleagle and Businger (1980). Quite simply, the net long wave radiative flux is given by:

$$F(long) = Fu - Fd \qquad (2.14)$$

where Fu and Fd represent the net upward and downward radiative fluxes, respectively.

Short wave radiative flux is calculated using the delta-Eddington method described by Joseph et al., (1976).

The solar flux is evaluated over 15 equally spaced (.1um) bands ranging from 0.2 to 1.7 um wavelength. Solar zenith angle as determined from previously described input variables is an essential part of these calculations. Several considerations are essential in modeling shortwave radiative flux. Shortwave extinction is primarily a result of scattering (instead of absorption). Scattering which creates a diffuse source of radiation is due to atmospheric particles, water droplets (in the case of clouds) and sea aerosols. The MABL incorporates the direct and diffuse sources of shortwave radiation in determining the total surface flux. Sea surface reflection of incident shortwave radiation is assigned a value of 10 percent.

Due to the one dimensionality of the model and several assumptions incorporated in the Q method of subsidence determination, atmospheric advection was assigned a value of zero.


D. OCEANIC BOUNDARY LAYER MODEL (OBL)

The OBL model was developed by Garwood (1977). It is a one dimensional, second order bulk model. The model employs the Navier-Stokes equation of motion with the geostrophic component eliminated, the continuity equation (assuming incompressible water), the heat equation derived from the first law of thermodynamics, a nonlinear equation of state and the conservation of salt equation.

The dynamics of the entrainment process determine the rate of deepening or shallowing (retreat) of the mixed layer. The fundamental assumption is that the turbulence of the mixed layer provides the energy required to destabilize and erode the underlying stable water mass (Garwood, 1977). As a result, the turbulent kinetic energy budget provides

21

the basis for the determination of the entrainment rate.
The system of equations is closed via the mean turbulent
field modeling of the vertically integrated equations for
the individual turbulent kinetic energy components along
with the bulk buoyancy and momentum equations.

The OBL model differs from earlier efforts in the
following ways. First, the amount of wind generated turbu-
lent kinetic energy to be used in mixing is a function of
the ratio of the mixed layer depth to the Obukhov mixing
length. Also, viscous dissipation is dependent on a local
Rossby number and seperate vertical and horizontal equations
for turbulent kinetic energy are used (Garwood, 1977).

Buoyancy conservation employed in the OBL is a generali-
zation of the concepts of heat and salt conservation. The
buoyancy equation is a combination of a linearized equation
of state, conservation of heat and conservation of salinity
equations. Buoyancy is simply defined by:

$$\tilde{b} = (\rho_o - \tilde{\rho}) \, g / \rho_o \tag{2.15}$$

where $\tilde{\rho}$ is given by:

$$\tilde{\rho} = \rho_o \{1 - \alpha(\tilde{\theta} - \theta_o) + \beta(\tilde{S} - S_o)\} \tag{2.16}$$

and where $\tilde{\theta}, \tilde{S},$ and $\tilde{\rho}$ are instantaneous values of temperature,
salinity and density, $\alpha$ and $\beta$ are expansion coefficients for
heat and salt respectively. The zero subscript denotes a
constant, representative value.

Parameters required for OBL model initialization include
shortwave radiation absorbed from the ocean surface to a
depth of one meter, the radiation extinction coefficient for
determining the downward heat flux and the critical

22

Richardson number for a stability adjustment at the base of the mixed layer. Surface boundary conditions require specification of wind speed and direction data, cloud cover, sea surface temperature, dry bulb and dew point temperatures, incident solar radiation and precipitation (P) and evaporation (E) rates.

Bulk aerodynamic formulae are used to calculate the turbulent fluxes of latent heat (Qe) and sensible heat (Qh). Shortwave radiation is calculated as previously described (delta Eddington method). An empirical equation (Husby and Seckel, 1978) is used in the determination of the net back radiation, Qb. The upward heat flux is simply the sum of these fluxes:

$$Qu = Qe + Qh + Qb \qquad (2.17)$$

The net radiation is not simply the difference between the downward and upward fluxes since only a fraction of the incident radiation penetrates the mixed layer. The depth of penetration is a function of turbidity, that is, in coastal regions more energy will be absorbed than in the less turbid, open ocean regions. The fraction of shortwave radiation which is absorbed is conceptually regarded as a contribution to the upward radiation. Therefore, the net heating at the surface is represented by:

$$Qnet = Qu + Rf(Qs) - Qs \qquad (2.18)$$

where Rf is the fraction of incident radiation absorbed in the first meter.

Given Qnet the surface fluxes of buoyancy and momentum can be calculated. At this point the turbulent fluxes of buoyancy, salinity and temperature can be determined by:

23

$$b'w' = g\{\hat{\alpha}(T'w') - \beta(s'w')\} \qquad\qquad (2.19)$$

$$s'w' = (P-E)So \qquad\qquad (2.20)$$

$$T'w' = -Qnet/\rho Cp \qquad\qquad (2.21)$$

where So represents a surface salinity.

Temperature and salinity profiles as well as the wind driven horizontal current profiles are required for OBL model initialization. Temperature is considered to be the dominant factor in density variation when compared to the effects of salinity over relatively short time periods such as those encountered in this study (Miller, 1976). The initializing profiles are used in the determination of mixed layer depth. According to the OBL model, mixed layer depth is defined to be the shallowest depth at which the observed density value $\sigma t$, is $.025\sigma t$ units greater than the density at the surface.


E.  COUPLED BOUNDARY LAYER MODEL

The processes outlined in the preceding sections have been combined to form a coupled boundary layer model. The coupling is achieved by matching the atmospheric and oceanic fluxes of momentum, sensible and latent heat and radiation at the air-sea interface, O'Laughlin (1982).

The only oceanic variable which forces the atmospheric model is sea surface temperature. Feedback occurs between several atmospheric variables and sea surface temperature. These include wind stress and the fluxes outlined previously. Conversely, nearly all of the atmospheric variables influence the evolution of the oceanic variables.

## 1.  Model Initialization

Coupled model initialization requires the Julian date, local time of day and latitude. Required atmospheric variables are surface pressure, inversion height, LCL, and mixed layer values of specific humidity and potential temperature. Also required are the inversion "jump" values and above layer lapse rates of potential temperature and specific humidity, vertical velocity (subsidence), and values for temperature and moisture advection. The 10 meter wind direction is also specified. The atmospheric model simply requires wind speed; however, the wind stress calculations needed for the OBL require the direction from which the wind is blowing. These computations lead to the determination of ocean turbulent velocity flux $U*^2$ where:

$$\tau_s = \rho_a U*^2 = \rho_w U_w*^2 \qquad\qquad (2.22)$$

Oceanic variables required for initialization are mixed layer depth, sea surface temperature, temperature jump value at the thermocline and the below layer thermal gradient.

Since atmospheric processes occur on a shorter time scale than oceanic processes, the MABL model is designed with a 30 minute time step whereas the OBL model uses a 60 minute time step. It is assumed that sea surface temperature will not change significantly over a 60 minute period. As a result, the ocean model is incorporated as a subroutine of the atmospheric model and is called every other time step. A schematic of the coupled model is depicted by Fig. 2.3.

25
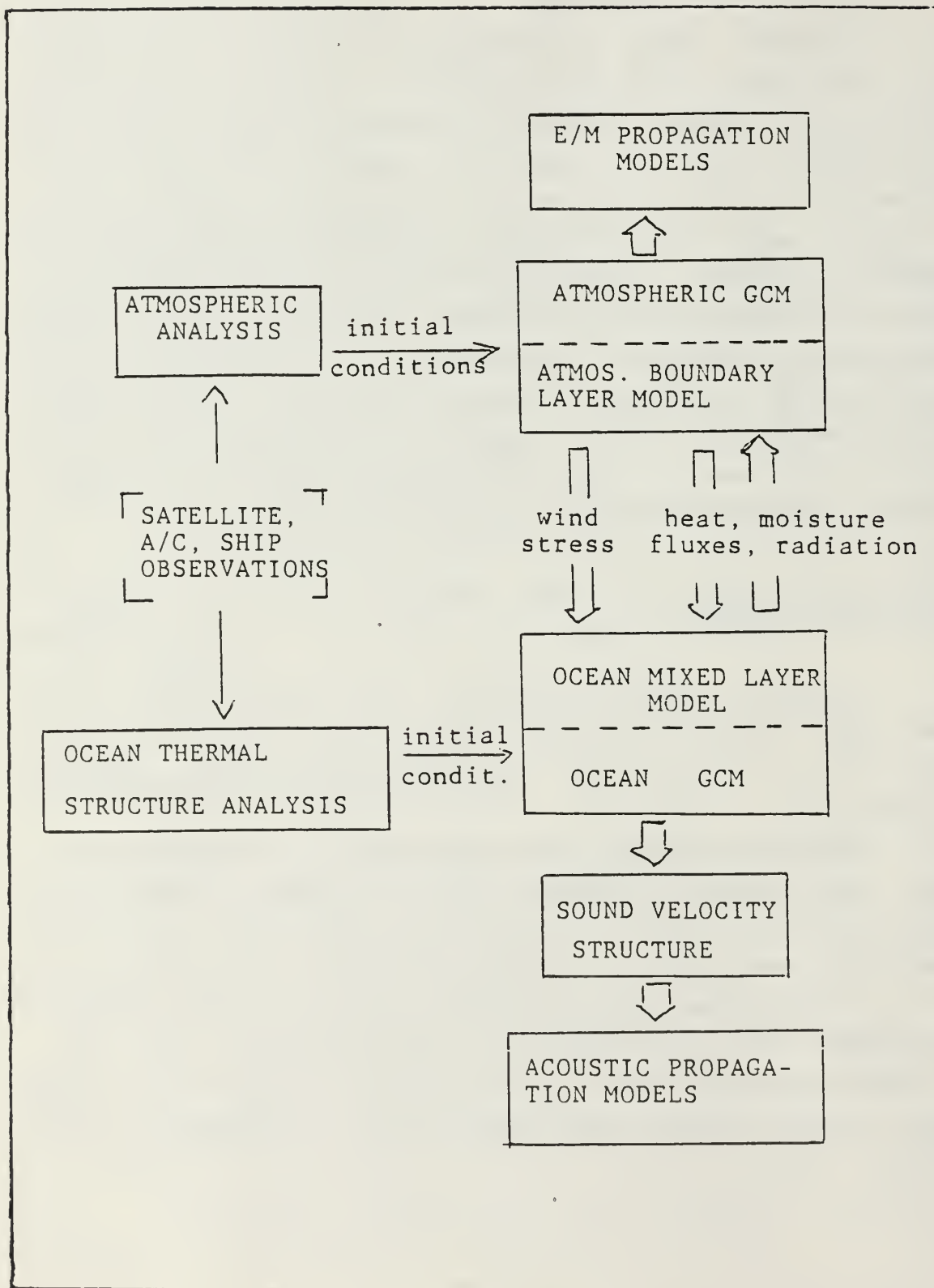
Figure 2.3    Coupled Model Schematic

26

# III. OBSERVATIONS AND RESULTS

## A. APPROACH

The data used in this study are from the Mixed Layer
Dynamics Experiment (MILDEX), conducted in the Eastern
Pacific from 24 October to 10 November 1983. Several
criteria were used in selecting the periods for which a
sensitivity analysis could be conducted. These included an
absence of atmospheric fronts and the availability of
frequent and accurate radiosonde and CTD data. Frontal
effects; such as, moisture and heat advection are not
included in the coupled or uncoupled models. The presence
of such activity would therefore impair comparison of the
one-dimensional model computations with observed changes in
the ocean and the atmosphere in particular.

The necessity of frequent radiosonde and CTD data is
critical to the determination of the temporal variation of
atmospheric and oceanic variables. The radiosonde data had
to be calibrated using measured temperatures at 20 m, which
was assumed to be continually within the atmospheric mixed
layer. The measured temperatures were converted to poten-
tial temperature, assuming a hydrostatic balance. The
atmospheric model was then initialized with this potential
temperature profile. Several data transmission problems
limited the amount of acceptable radiosonde data.
Radiosonde launch times coincided with weather satellite
overhead time. This time resolution was insufficient to
resolve well any synoptic variability in the atmosphere.
Oceanic data required no post calibration. However, it too
was limited in continuity due to equipment malfunction. As
a result, two periods were selected for this analysis.

The first period began at 1600 (Pacific Daylight Time) 03
November and concluded at 1554 04 November. The second
period began at 1554 04 November and concluded at 1600 05
November. The data selection process is outlined in Fig.
3.1.
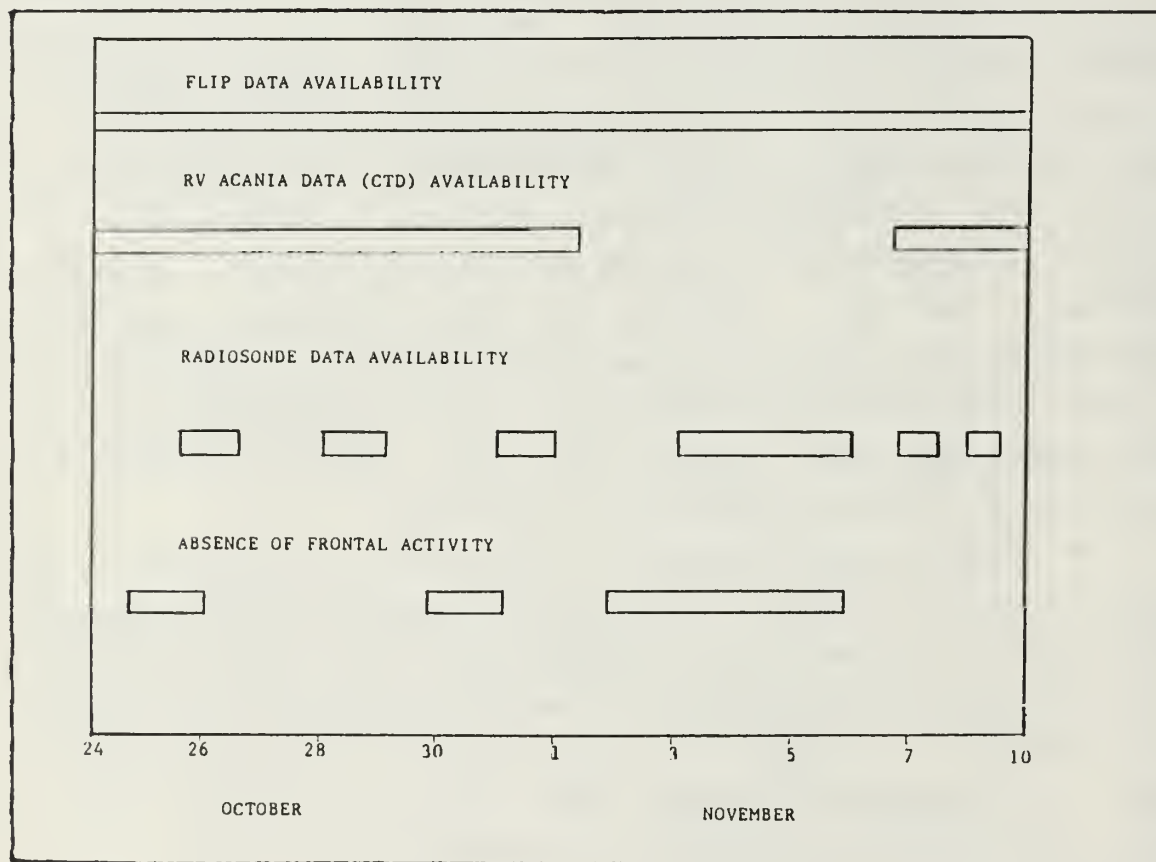


Figure 3.1 Period Selection Criteria

Initial model values for the atmospheric mixed layer,
inversion jump and above layer lapse rates for potential
temperature and specific humidity were obtained from radio-
sonde data. Sequential atmospheric soundings were used to
determine subsidence rates. Methods for determining subsi-
dence using mean values as well as least squares values are
available. Significant differences were not found for the

different approaches; thus, the mean value method was employed in model initialization. Sequential radiosonde profiles preceding and including the profile at the begining of each experimental period were used in subsidence calculations. The remainder of the atmospheric variables required in initialization were tabulated by Geernaert et al., (1984), with the exception of LCL. This value was determined through the use of a Skew T, log P diagram.

Oceanic variables required for initialization were determined from temperature profiles from CTD casts. Mixed layer depth, temperature jump at the thermocline and below layer gradients were thus obtained. The overlapping of oceanic data from ACANIA CTD measurements and FLIP provided a temporally complete data set.

## B. CASE I: 1600 PDT 03 NOVEMBER-1554 04 NOVEMBER 1983

### 1. Uncoupled Model

The values used to initialize Case I are listed in Table I. The uncoupled and coupled model predictions are presented in Figs. 3.2 and 3.3 respectively. In terms of the evolution of the inversion height and LCL, the uncoupled model began with a cloud layer (15 m thickness) with a base at 266 m. Within two hours, the LCL decreased rapidly (from 266 to 126 m) as the inversion height rose. The result was an extremely thick cloud which attained a maximum thickness of 635 m with a base at 183 m, at 0500.

The decrease of the LCL was a result of a combination of factors. The specific humidity increased slightly after initialization followed by a very gradual decrease (.56 g/kg) through 0200. Air temperature decreased $1.9^{\circ}C$ from 1600 through 0300. As a result, the air-sea temperature difference increased since the sea surface temperature was held constant. The increase in air-sea temperature
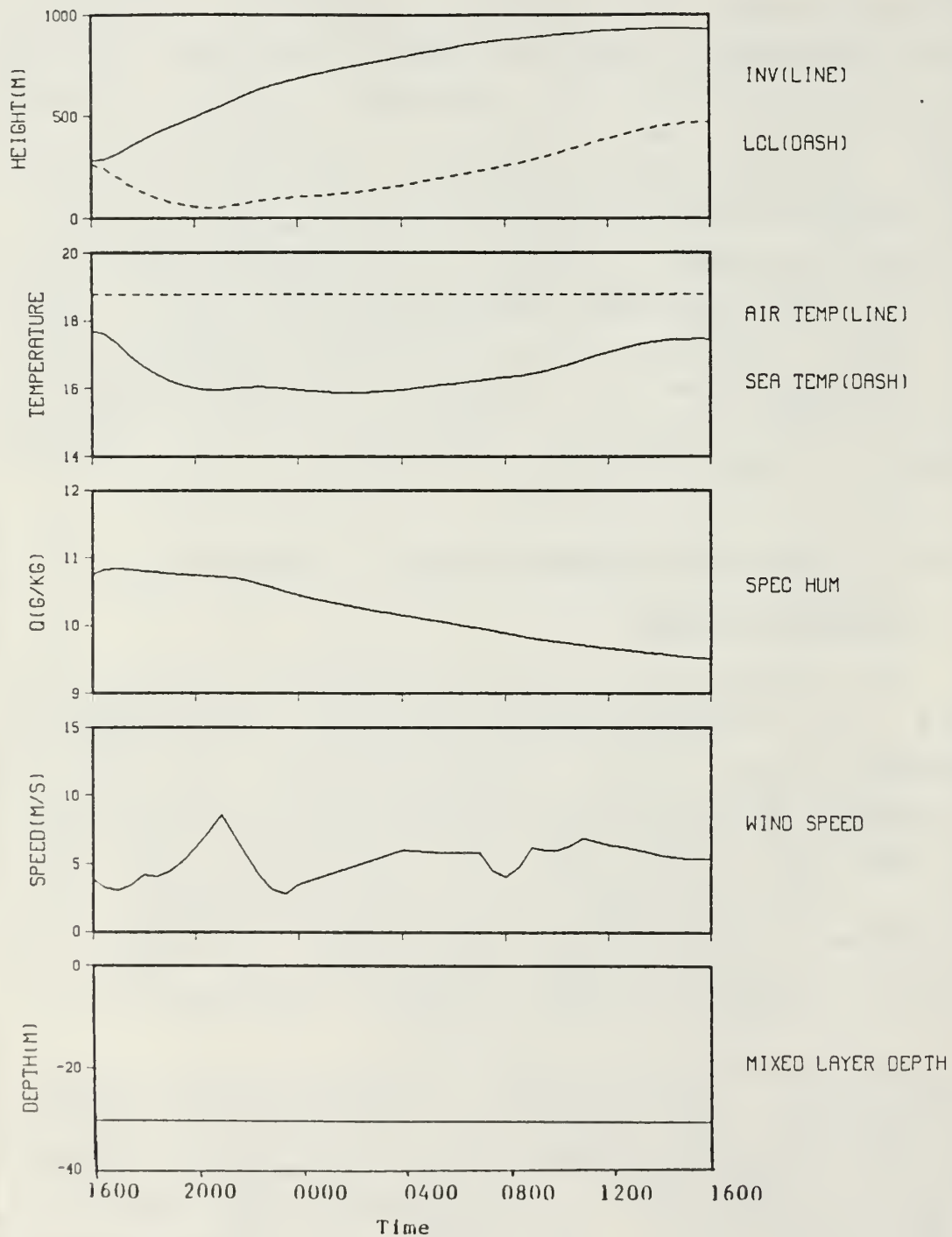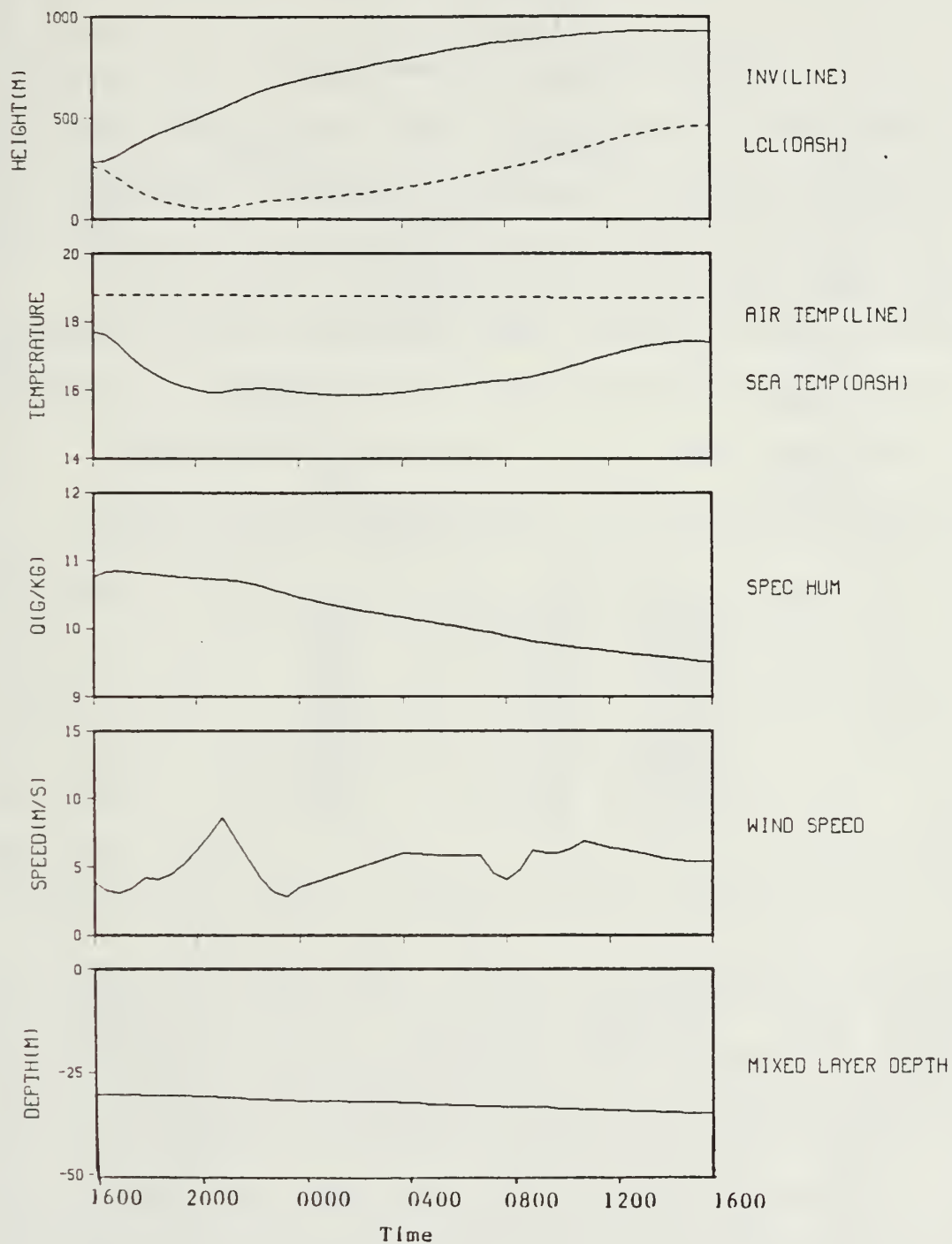
29

Figure 3.2    Uncoupled Model-Case I

30

Figure 3.3    Coupled Model-Case I

31

```
                            TABLE I
                  Initialization Values-Case I

      Julian Date       Sfc Pressure (mb)    Sea Sfc Temp (°C)
          307               1022.4                18.78

      Inversion Ht (m)     Mixed Layer Potential Temp (°C)
          281                        17.70

      Air Temp Jump (°C)     Temp Lapse Rate (°C/m)
          1.5                        .0067

      Spec Humidity (g/kg)     Spec Humidity Jump (g/kg m)
          10.75                        -.31

      Spec Humidity Lps Rate (g/kg m)        LCL (m)
          -.0035                              849

      Subsidence (m/s)            Mixed Layer Depth (m)
          -.0032                            30

      Ocean Temp Jump (°C)    Ocean Temp Gradient (°C/m)
          -.2                         -.0174

              Wind: Time    Speed (m/s)    Dir (°T)
                    1600      3.9            040
                    1802      4.2            319
                    2105      8.6            036
                    0017      3.5            288
                    0417      6.0            276
                    0722      5.8            293
                    0922      6.2            028
                    1123      6.9            342
                    1340      6.1            001
                    1541      5.4            340
```

difference is reflected in a continuous increase in moisture flux. Following sunrise, the air temperature increased associated with a decrease in specific humidity, a less rapid increase of moisture flux and an elevation of the LCL.

The inversion height increased throughout the prediction period. The time rate of change of this parameter is the difference between the rates of entrainment and subsidence. Entrainment rate reached a maximum value of 2.3 cm/s at 2130 and decreased slightly to a value of 1.5 cm/s

at the end of the period. Subsidence was held constant at a value of -.0032 m/s throughout the period. This value is representative for subsidence in this region as noted by Davidson et al., (1984). As a result, the evolution of the inversion height was dominated by the rate of entrainment. The entrainment of warm, dry air into the mixed layer also contributed to the gradual decrease of specific humidity and the increase in air temperature observed prior to sunrise.

Sea surface temperature and mixed layer depth remain constant with the uncoupled model execution i.e. no ocean variability is permitted.

2. Coupled Model

The uncoupled and coupled models predicted nearly identical atmospheric results. Clouds were present from the beginning of the period. Cloud thickness and the evolution of the LCL and inversion height remained the same as in the uncoupled model. Air temperature and specific humidity profiles were also unchanged. The coupled model determines sea surface temperature hourly. Therefore, the air-sea temperature difference, moisture and temperature fluxes would be expected to vary. In this case, the sea surface temperature decreased from an initial value of 18.78 $^{\circ}$C to 18.69$^{\circ}$C, a change of only .09$^{\circ}$C. As a result, the time rate of change of moisture and temperature fluxes for the coupled and uncoupled models is nearly identical. Sea surface cooling results in convective mixing (negative buoyancy flux), cooling throughout the layer, and an increase in mixed layer depth for both the atmosphere and ocean. The impact of the ocean upon the atmospheric mixed layer processes is almost invariant in this case. The major influence upon the atmospheric mixed layer is the inversion height growth and associated entrainment.

33

## C.  OBSERVATIONS VS MODEL OUTPUT

Observed specific humidity compares favorably with model output, Fig. 3.4.  The time series are nearly identical eight hours following initialization.  From 12 to 18 hours after initialization the observed specific humidity shows an increase of approximately 1.0 g/kg.  The model predicted a continuous decrease throughout the period.  As the end of the period is approached, the model and observed specific humidity differ by less than .5 g/kg.
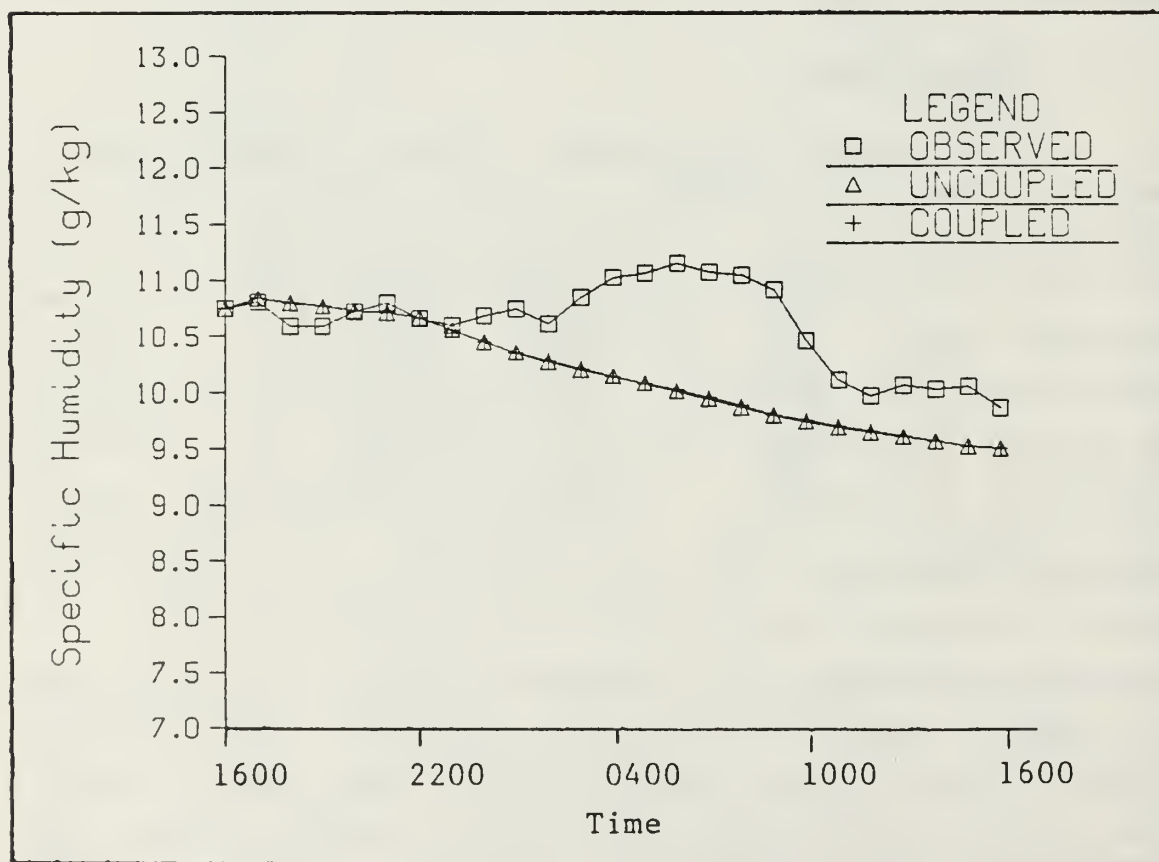


Figure 3.4    Specific Humidity
Observed vs Model (Case I)

The model prediction of air temperature differs by as much as 2°C from observed values from 2000 to 0400, Fig.

34
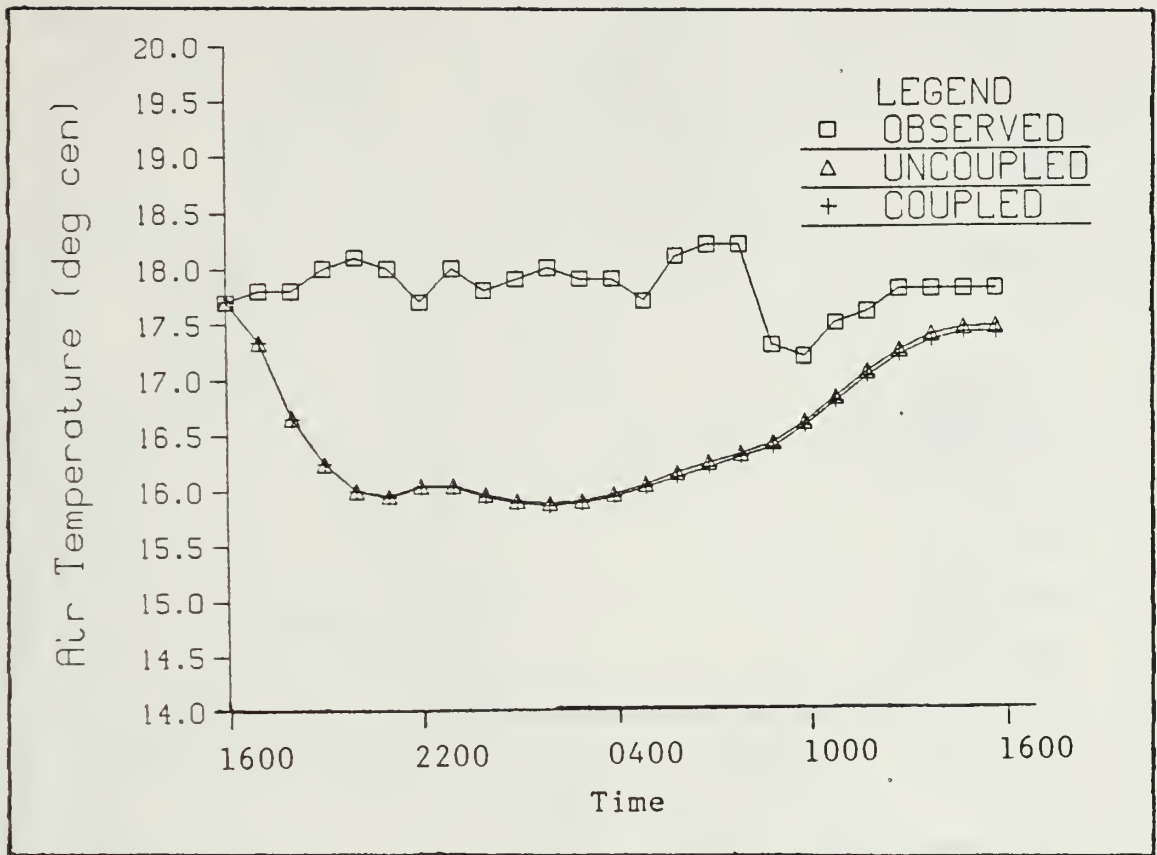
Figure 3.5    Air Temperature
Observed vs Model (Case I)

3.5.    From 1000 to the end of the period,  the observations
and  predictions  demonstrated an  increase  and  eventually
attained a constant air temperature,  differing by less than
$0.5°C$.    The large difference in  air temperature (ca.   $2°C$)
which occurs was a result of thick cloud cover and resultant
shortwave radiation deficit.

    There  were vast  differences  in  observed and  modeled
shortwave radiation, Fig.  3.6.    The radiation for a cloud
free case  verifies that  there was  a cloud  cover present.
This  result is  deduced from  the  difference in  shortwave
radiation  between the  cloud  free  case and  the  observed
values.    Clouds were  present from  15 to  20 hours  after

35
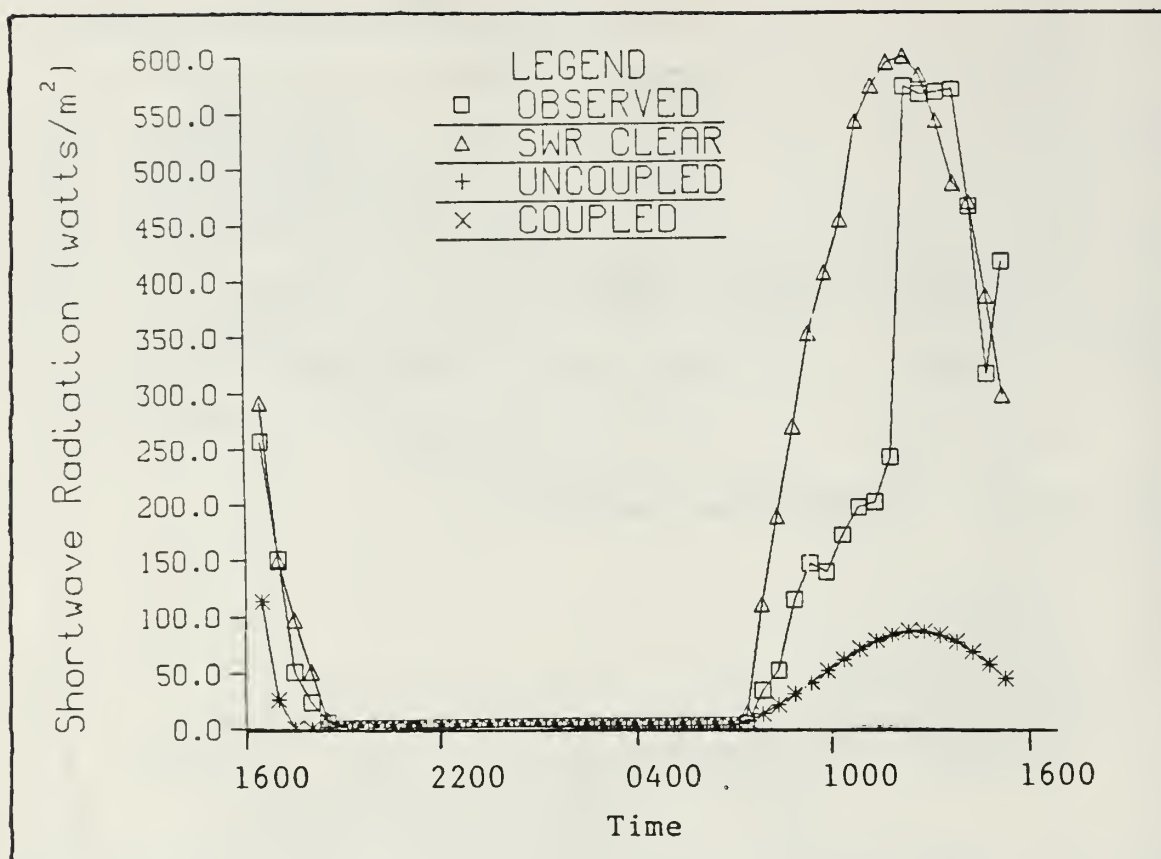
Figure 3.6    Shortwave Radiation
Observed vs Model (Case I)

initialization.   Uncoupled and coupled model calculations of
shortwave radiation are closely correlated.    However,  they
are substantially  smaller than the observed  values.    This
difference is a   result of the assumption   of complete cloud
cover when the LCL is beneath the inversion height.   Horizon
to horizon cloud cover will result in a fractional amount of
shortwave radiation in comparison with  a variable amount of
cloud cover.

The effect   of the  over prediction  of cloud  cover has
been   addressed   previously.    The   cooler   air · temperature
determined by the  model and the cooling of  the sea surface
and deepening  of the mixed layer  by the coupled  model are
two examples.   These differences impact variables such as

specific humidity and LCL, which are functions of air
temperature. These variables are fundamental to the deter-
mination of the rate of change of all of the model parame-
ters.
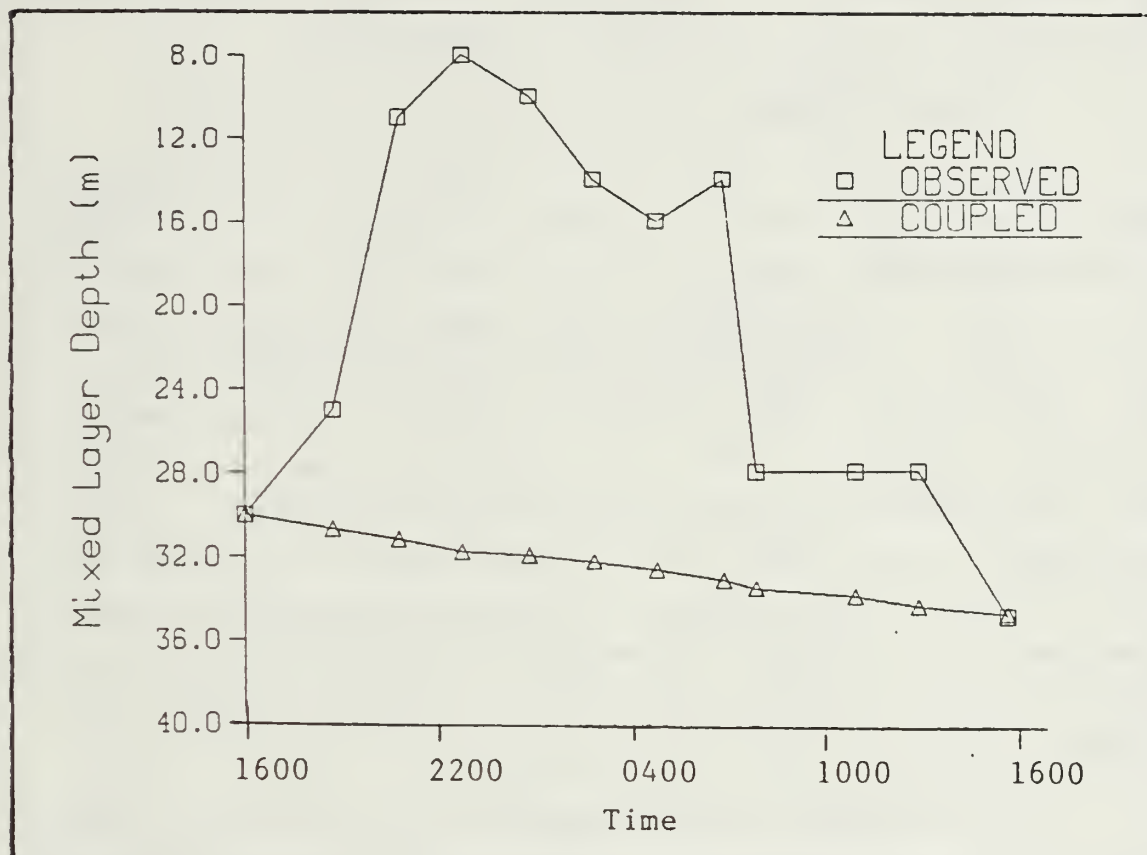


Figure 3.7    Mixed Layer Depth
Observed vs Model (Case I)

Observations indicated a shallowing of the mixed layer
from 1900 through 2300, Fig. 3.7. This was followed by a
gradual deepening. It is due to the surface heating and the
distribution of heat by wind mixing followed by radiative
cooling and convective overturning. The model predicted a
continuous deepening of the mixed layer due to the substan-
tially reduced values of shortwave radiation and the resul-
tant sea surface cooling and convective instability.

37

D. CASE II: 1554 PDT 04 NOVEMBER-1600 05 NOVEMBER 1983

The initializing variables for the second 24 hour period are listed in table II. Uncoupled and coupled model outputs are presented in Figs. 3.8 and 3.9 respectively.

1. Uncoupled Model

In this case, (Fig. 3.8), the cloud development is less extreme than that which arose in Case I. A cloud of minimum thickness formed when the model was initiated (20 m). As the run progressed, the model determined a fairly constant LCL, whereas inversion height increased rapidly from 1600 through 1900 (492 to 768 m). The inversion attained a height of 1093 m at 0630 and remained at this level until 1030, at which time it began to lower. At the conclusion of the model run the inversion had dropped 23 m from its maximum of 1093 m. The LCL decreased slightly throughout the period. It began at a level of 472 m and reached a final height of 422 m. The cloud thickness had a maximum of 701 m at 0930, 05 November.

The behavior of the inversion is reflected in the modeled entrainment rate. As the inversion height increased in the early portion of the period, entrainment rate attained an absolute maximum value of 3.68 cm/s. Thereafter, the predicted rate of entrainment decreased, ultimately attaining a value of .679 cm/s. The final value represented an absolute minimum. Since the prescribed subsidence rate was held constant, the rate of entrainment again dominated the evolution of the inversion height.

The LCL remained relatively constant throughout. This was a result of the compensating effects of dry air entrainment and an increasingly larger air-sea temperature
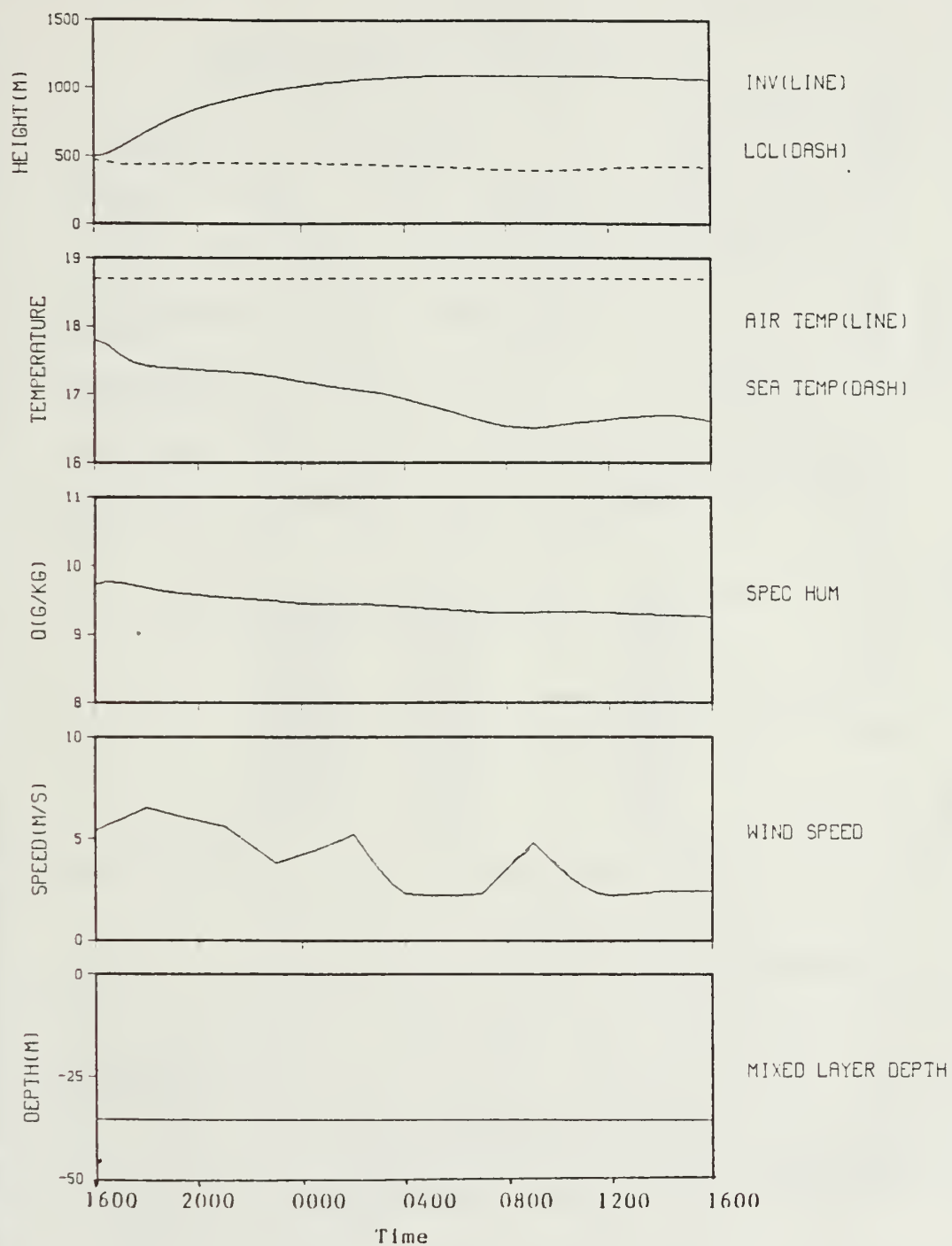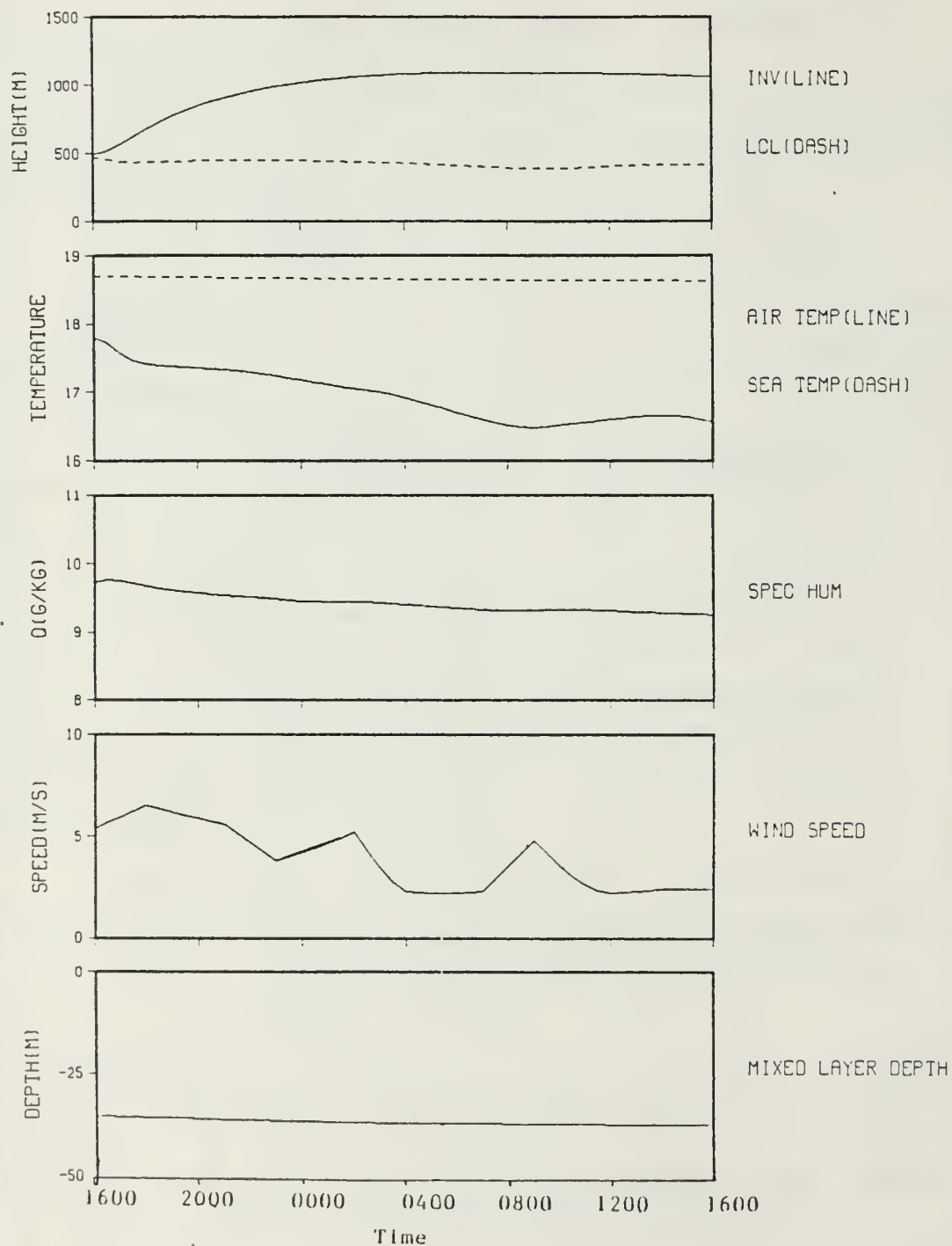
Figure 3.8    Uncoupled Model-Case II

39

Figure 3.9    Coupled Model-Case II

```
                        TABLE II
              Initialization Values-Case II

   Julian Date      Sfc Pressure (mb)    Sea Sfc Temp (°C)
       308               1022.3              18.70

   Inversion Ht (m)     Mixed Layer Potential Temp (°C)
       492                     17.80

   Air Temp Jump (°C)    Temp Lapse Rate (°C/m)
       1.5                    .0065

   Spec Humidity (g/kg)    Spec Humidity Jump (g/kg m)
       9.72                      -.94

   Spec Humidity Lps Rate (g/kg m)      LCL (m)
       -.0017                           1079.12

   Subsidence (m/s)              Mixed Layer Depth (m)
       -.0039                            35

   Ocean Temp Jump (°C)    Ocean Temp Gradient (°C/m)
       -.2                           -.1411

            Wind:  Time    Speed  (m/s)    Dir (°T)
                   1600     5.4             340
                   1830     6.5             340
                   2100     5.6             351
                   2330     3.8             345
                   0200     5.2             325
                   0430     2.3             016
                   0700     2.3             344
                   0930     4.8             333
                   1200     2.2             270
                   1430     2.4             265
```

difference.   The former would force an increase in the LCL,
the latter a decrease.   This balance is also evident in the
nearly constant predicted specific humidity values.   As the
moisture flux into the layer increased (due to the
increasing air-sea temperature difference) the incorporation
of dry, warm air (entrainment) resulted in a slight varia-
tion in specific humidity.

Air temperature in the mixed layer, if viewed in
terms of radiative heating and cooling, would be expected to
decrease after sunset and increase after sunrise.   This is

the case as shown in Fig. 3.8. The modeled shortwave radia-
tion is again underestimated. As a result, a significant
decrease in air temperature occurred through 16 hours into
the period due to cloud top long wave radiation.


2. Coupled Model

As observed in Case I, the coupled and uncoupled
model predictions are essentially identical in this case.
The coupled model prediction demonstrated a decrease in sea
surface temperature and a deepening of the mixed layer. Sea
surface temperature decreased from 18.7 to 18.63 °C. The
moisture flux decrease, due to the reduced sea temperature,
was too small to force any appreciable change in specific
humidity or LCL. The deepening of the mixed layer from an
initial depth of 35 to a 37.4 m had no effect upon the
atmospheric boundary layer.

While Case I and Case II experienced similar
decreases in sea surface temperature, the former deepened
the mixed layer by a factor of two greater than the latter.
However, friction velocity was larger in Case I than Case
II. Therefore, the variation of the mixed layer depth was
in response to wind forcing.

3. Observations vs Model Predictions

The predicted and observed specific humidity were
significantly different, Fig. 3.10. There is no difference
between coupled and uncoupled predictions as they exhibit a
slight decrease throughout the period. Observed specific
humidity varied in a cyclical fashion due to the relative
humidity variation.

Values of specific humidity were calculated exter-
nally using air temperature, pressure and relative humidity.
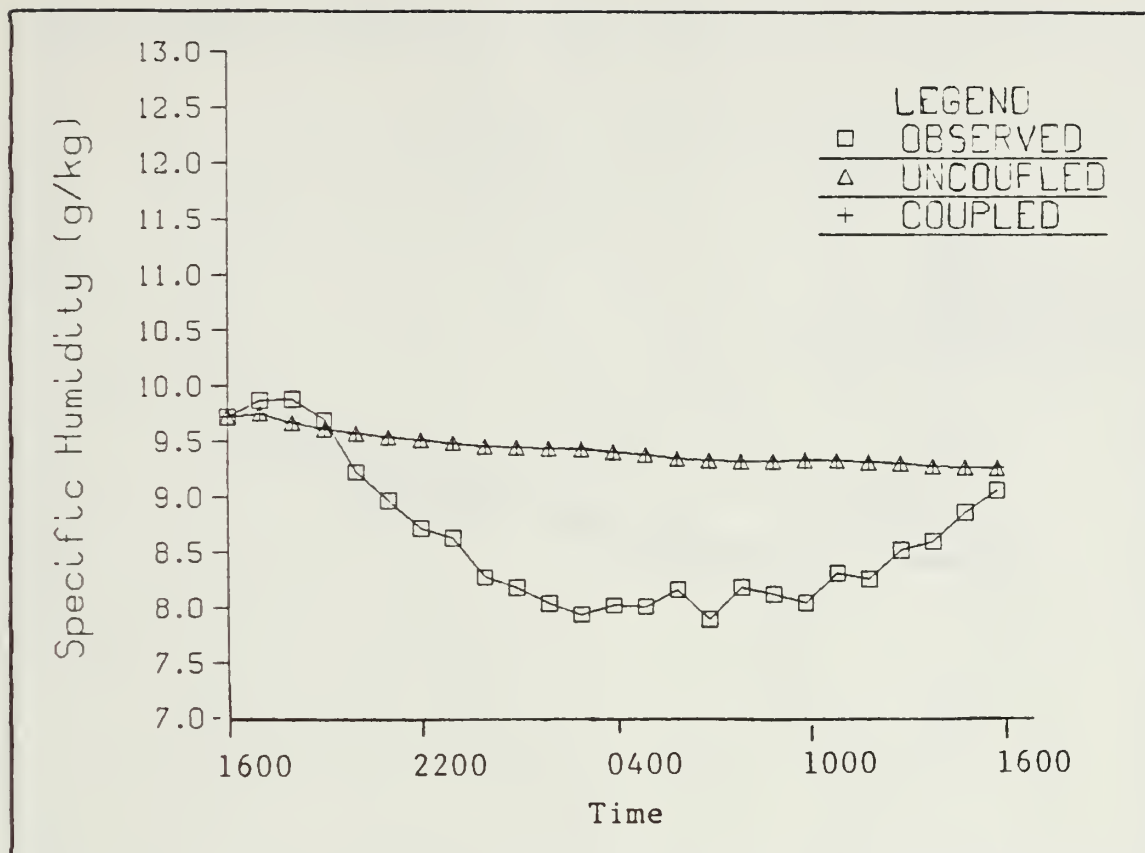Unlike Case I, a large decrease in relative humidity was

Figure 3.10    Specific Humidity
Observed vs Model (Case II)

experienced.    Specific  and relative  humidity changes  are
forced by surface moisture flux and entrainment.    Since the
predicted  and   observed  values for  air  and  sea  surface
temperature are nearly the same,  the difference lies in the
entrainment.    As noted  earlier,   the  predicted rate  of
entrainment decreased through the   period.    Actual entrain-
ment must  have increased during the  middle of the  run and
decreased at the end.

The radiosonde data (Fig. 3.11) support the observed
decrease  in mixed  layer specific  humidity.   Mixed  layer
specific humidity begins at a value of 9.76 g/kg,  decreased
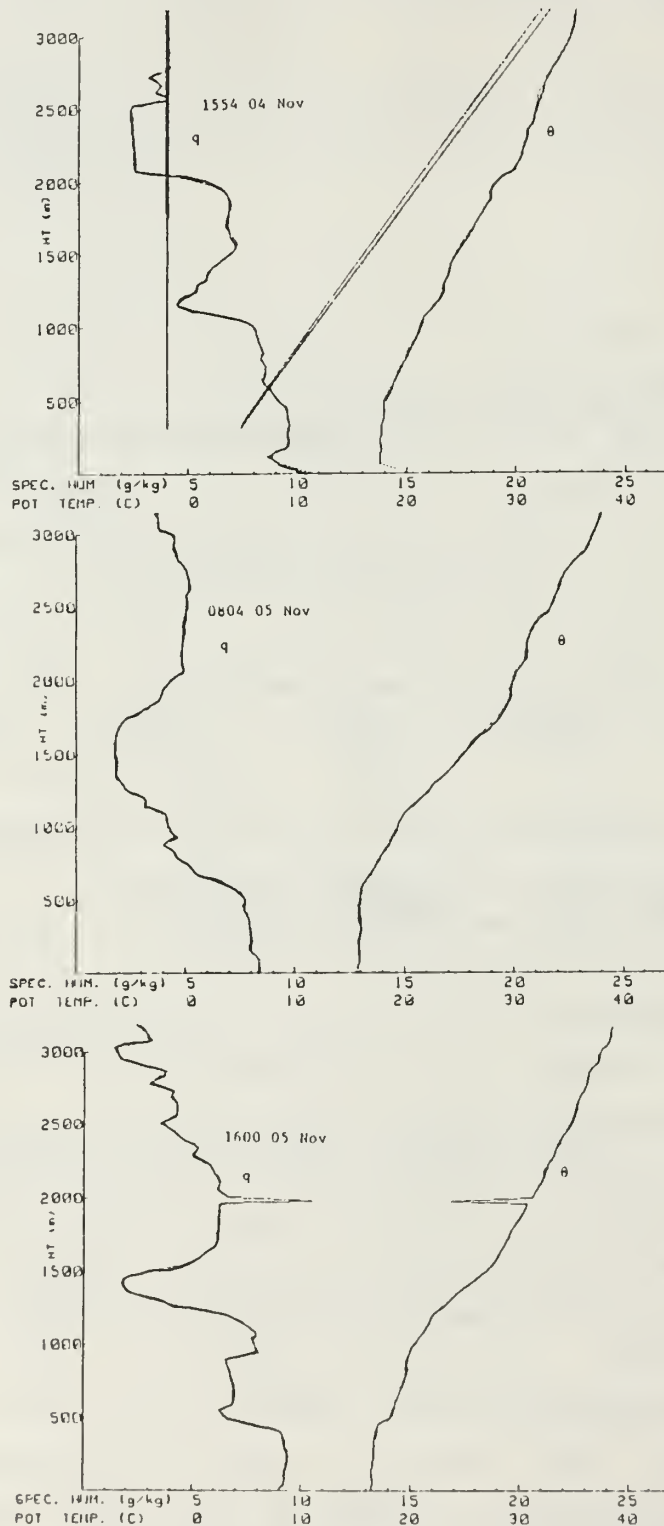to 7.84 g/kg  16 hours later,  and attained a  value of 8.98

43

Figure 3.11    Radiosonde Profiles

44

g/kg 24 hours into the period. The predicted entrainment
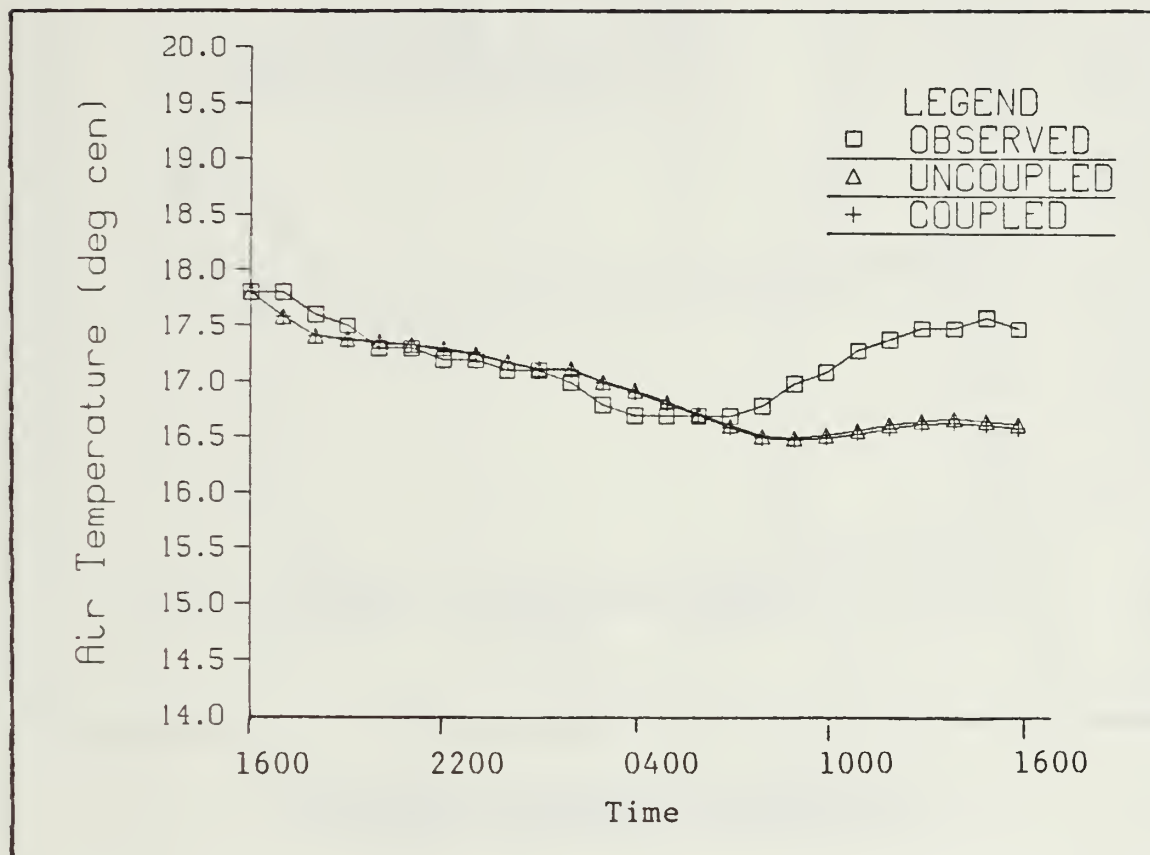is, therefore, smaller than that observed.



Figure 3.12    Air Temperature
Observed vs Model (Case II)

The air temperature was in close agreement for
observed, uncoupled and coupled cases exists 16 hours into
the period, Fig. 3.12. From this time, the predicted values
increase slightly while the observed air temperature
increases by greater than $0.5^{\circ}C$. At the end of the period a
temperature difference of $0.86^{\circ}C$ exists.

Predicted sea surface temperature agrees with
observed values 20 hours into the run, Fig. 3.13. The
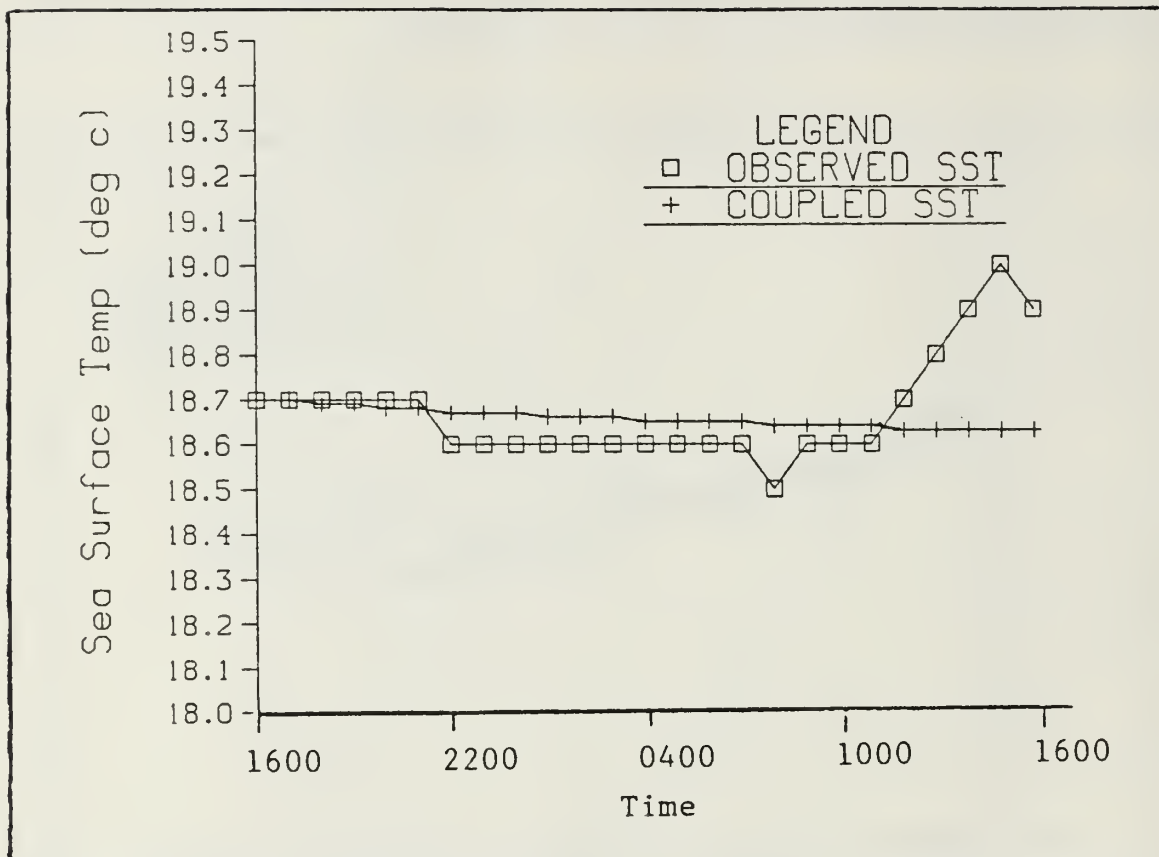observed sea surface temperature increased $0.3^{\circ}C$ from 16 to

Figure 3.13    Sea Surface Temperature
Observed vs Model (Case II)

24 hours after initialization (1200 to 1600 local time)  due
to shortwave radiative heating.   Predictions fail to demon-
strate this  increase due to  the extensive cloud  cover and
associated shortwave radiation deficit.    This dichotomy is
absent in  the early stages of  the run since the  model was
initialized with the observed sea surface temperature.

        Shortwave radiation  is again  underestimated,  Fig.
3.14.  A clear sky was observed as depicted by the agreement
of observed  and clear  sky values  of shortwave  radiation.
The model predicted a thick cloud layer and assumed  horizon
to horizon coverage.   This prediction   resulted in a severe
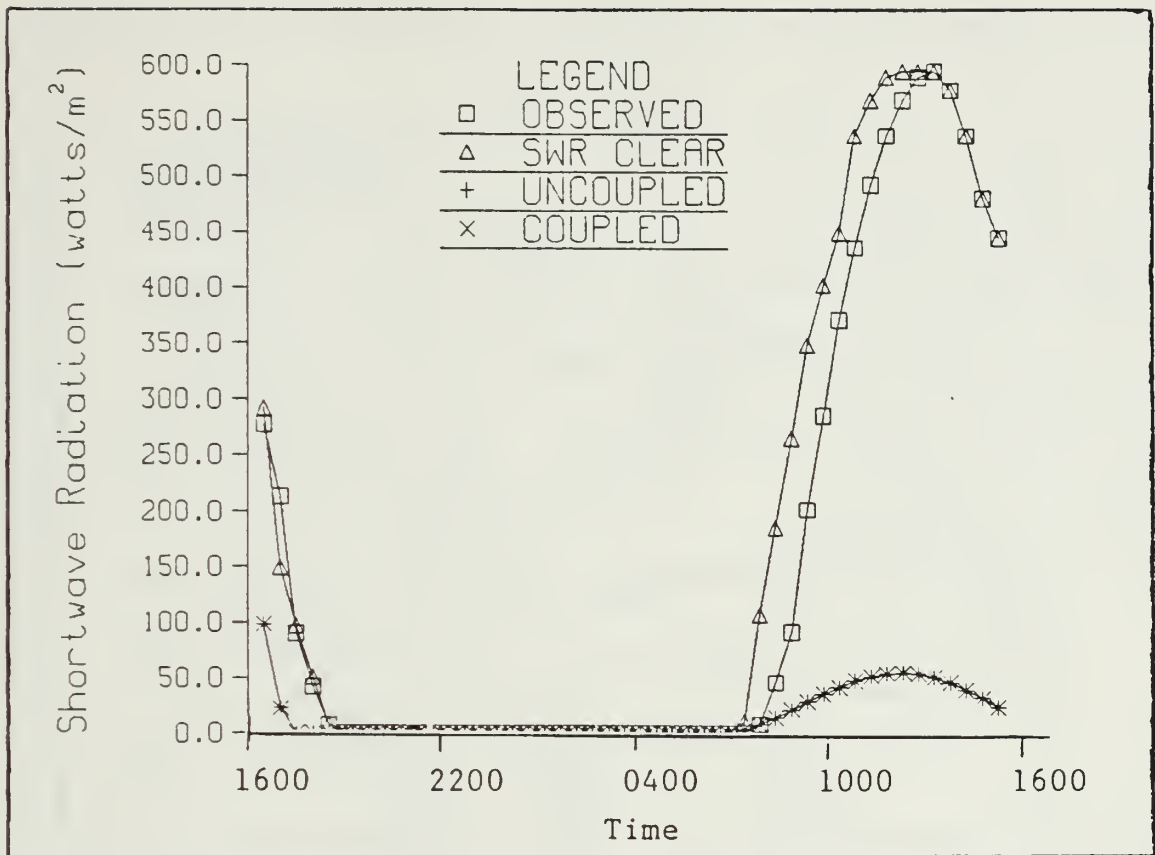underestimation of  shortwave radiation at the  sea surface.

Figure 3.14    Shortwave Radiation
Observed vs Model (Case II)

As in Case I, the effects of this radiation deficit are wide ranging throughout the model.

Through the comparison cf coupled model and observed variations of the mixed layer depth, a periodic retreat of the mixed layer was observed, Fig. 3.15.    A minimum depth was attained eight to ten hours  after the maximum in short-wave radiation due to the delayed oceanic response to heating and the  relatively light winds forcing  the mixing. Additionally,  the effects  of tides and internal  waves are most likely present  as evidenced by the  periodic variation in  mixed layer  depth.    The  shortwave radiation  deficit forced a deepening of the  mixed layer,  which resulted from
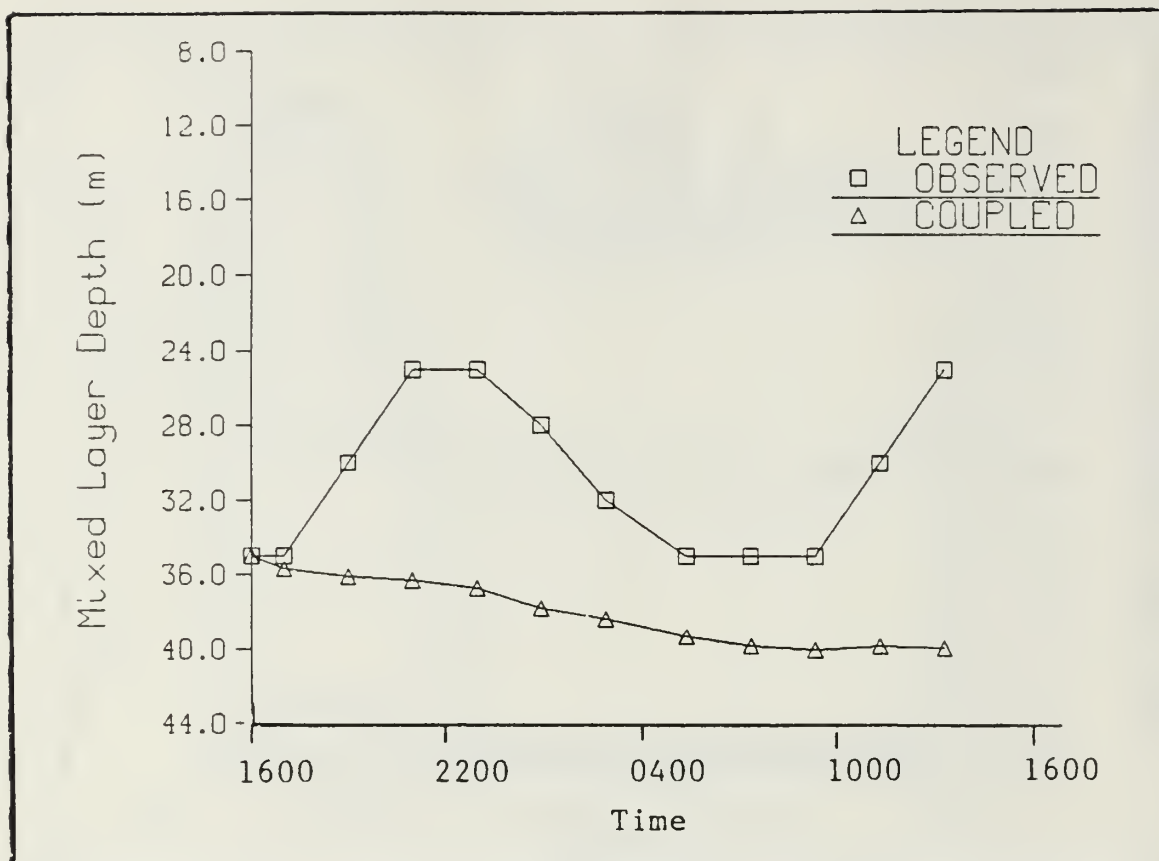
Figure 3.15    Mixed Layer Depth
Coupled vs Model

cooling of the sea surface and convective mixing.    This
pattern corresponds to the remainder of the modeled
variables.    However, it is significantly different than the
response of the ocean to the atmospheric forcing.


E.   CASE III: 1600 03 NOVEMBER-1600 05 NOVEMBER 1983

To compare model performance and observations for a
period greater than 24 hours, a 48 hour period was selected.
Due to the limitations imposed upon the experiment by the
environment and equipment malfunction,   the time frames for
Cases I and II were combined  to provide the longer forecast

```
                        TABLE III
              Initialization Values-Case III

   Julian Date      Sfc Pressure (mb)    Sea Sfc Temp (°C)
       308               1022.4               18.69

   Inversion Ht (m)     Mixed Layer Potential Temp (°C)
       928                       17.41

   Air Temp Jump (°C)     Temp Lapse Rate (°C/m)
       10.3                     .0065

   Spec Humidity (g/kg)    Spec Humidity Jump (g/kg m)
       9.52                     -3.8

   Spec Humidity Lps Rate (g/kg m)        LCL (m)
       -.0017                              417

   Subsidence (m/s)           Mixed Layer Depth (m)
       -.0032                         34

   Ocean Temp Jump (°C)    Ocean Temp Gradient (°C/m)
       -.2                         -.1411


        Wind: Time     Speed (m/s)     Dir (°T)
              1600        5.4            340
              1830        6.5            340
              2100        5.6            351
              2330        3.8            345
              0200        5.2            325
              0430        2.3            016
              0700        2.3            344
              0930        4.8            333
              1200        2.2            270
              1430        2.4            265
```

period.   The  output variables from  the last time  step of
Case  I were  employed  as  initializing variables  for  the
second  24 hour  period of  Case III.   These variables  are
listed in Table III.

The most obvious  difference in the Case  III prediction
as compared  with that  of Case  II was  that there  were no
rapid changes in  the predicted variables,  Figs.   3.16 and
3.17.    The  most  obvious  difference   in  the  Case  III
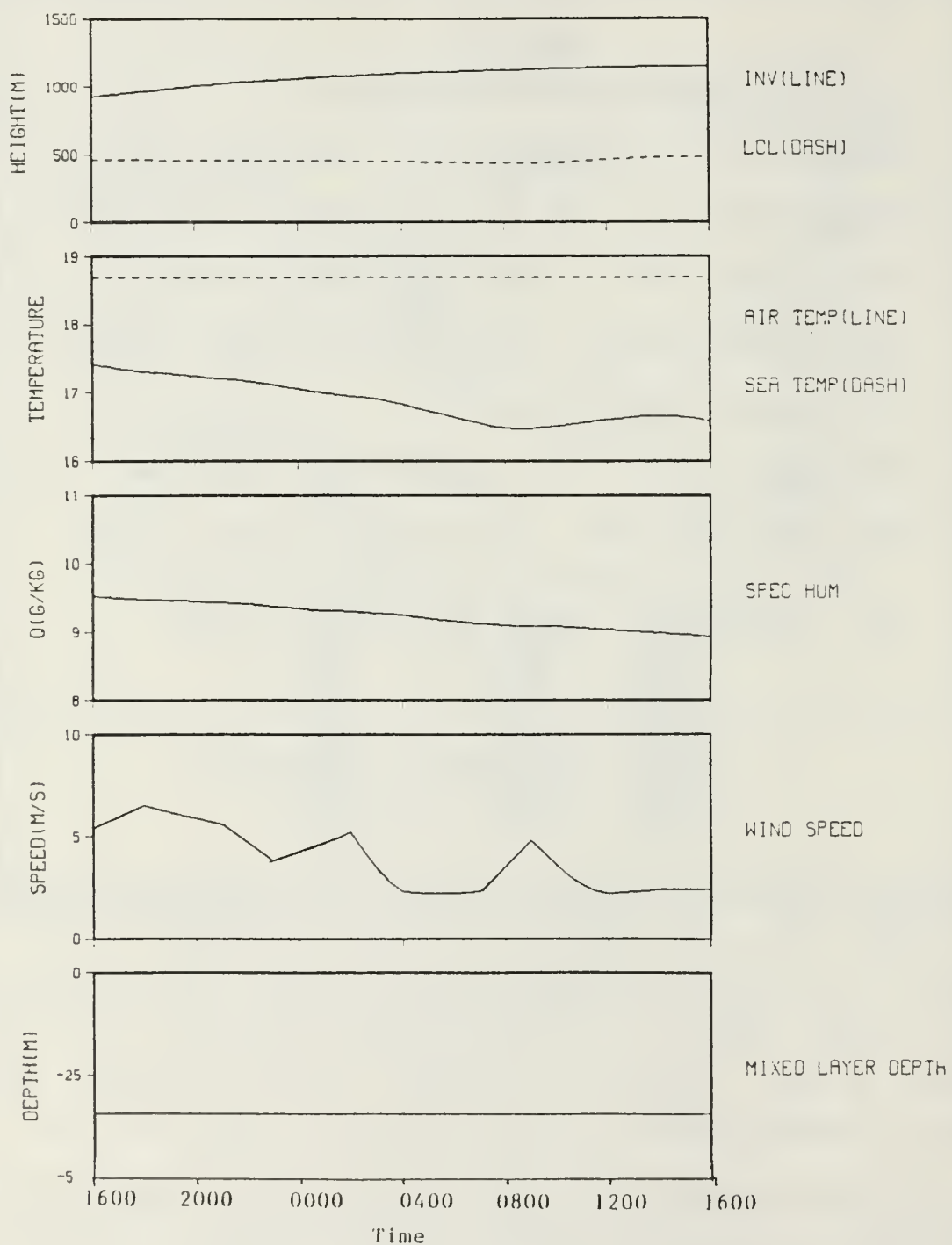prediction as compared  with that of Case II  was that there

49

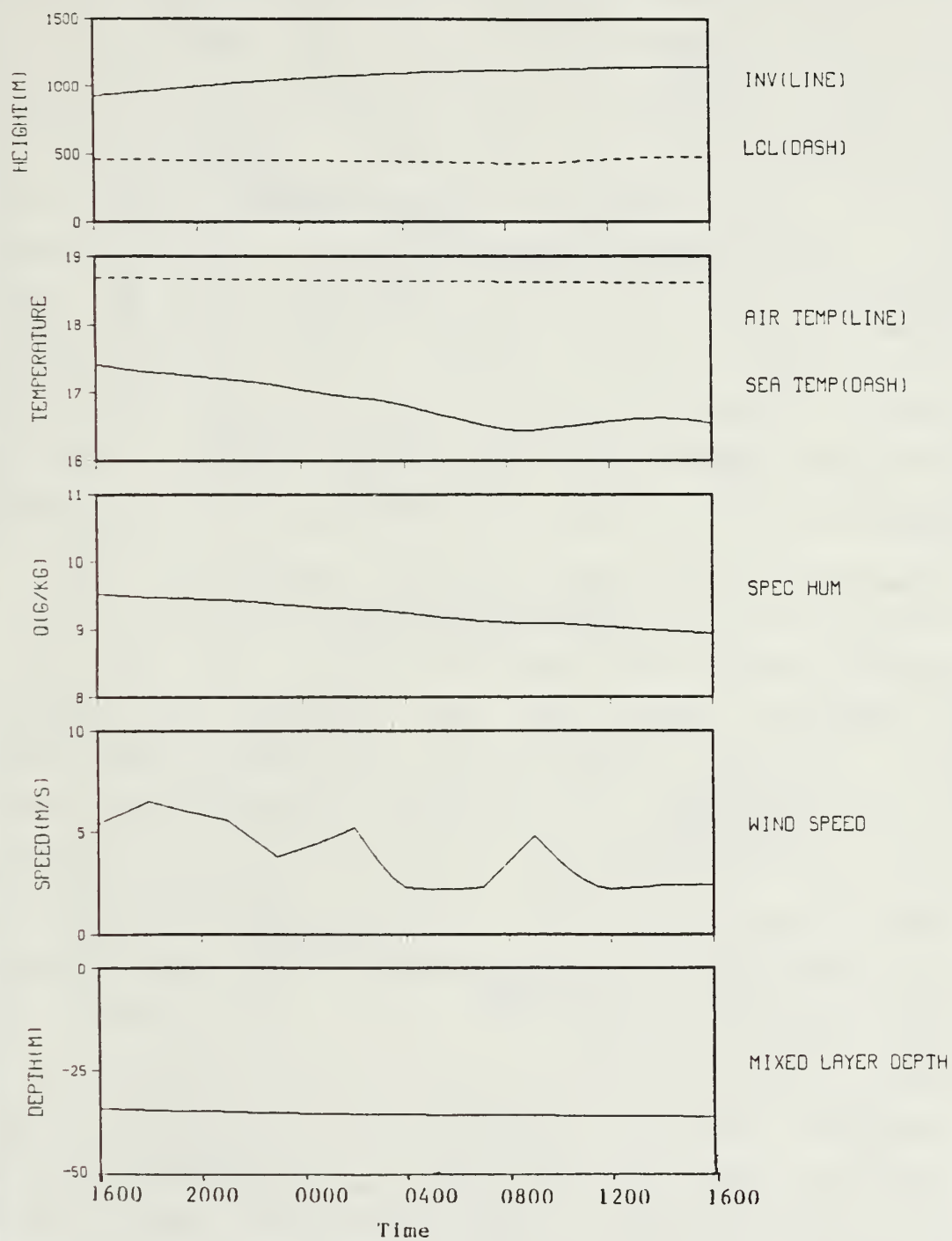Figure 3. 16    Case III Uncoupled Model

50

Figure 3.17   Case III Coupled Model

51

were no rapid changes in the output variables. The inversion height increased gradually from an initial value of 928 m to a final value of 1146 m. The LCL ranged from an initial value of 464 m to a minimum value of 438 m to a final height of 483 m. The LCL and inversion height attained final values of 424 and 1073 m, respectively, in Case II. Cloud thickness changed slightly during the period. It began at 464 m and increased to 663 m. Cloud thickness for Case II grew to a thickness of 649 m. The radiosonde soundings for the latter 24 hours period of Case III (Fig. 3.11) revealed the height of the inversion to be increasing. Though the profiles are not ideal, the final inversion base height is of the order of 1000 m. Hence, fairly good agreement exists for Cases II and III in this regard.

Temperature also varied gradually during the period. Both Cases II and III demonstrated a diurnal variation. Air temperature profiles are depicted in Figs. 3.18 and 3.19. Close agreement exists from the uncoupled and coupled models. There is essentially no difference between the output for these cases. The shortwave radiation deficit and associated lack of heating was obvious from 16 to 24 hours into the runs. An agreement of temperature values at the beginning of each run occurred as the result of initialization and because the runs began at 1600. Darkness occurred shortly thereafter. Thus there was a minimal amount of shortwave radiative heating.

A very close agreement in specific humidity resulted for both uncoupled and coupled models, and for the 24 and 48 hour periods, Figs. 3.20 and 3.21. As highlighted in the discussion of Case II the difference between observed and modeled specific humidities was due to an apparent increase in the actual rate of entrainment of warm dry air into the mixed layer, while modeled entrainment remained fairly constant and smaller in magnitude.
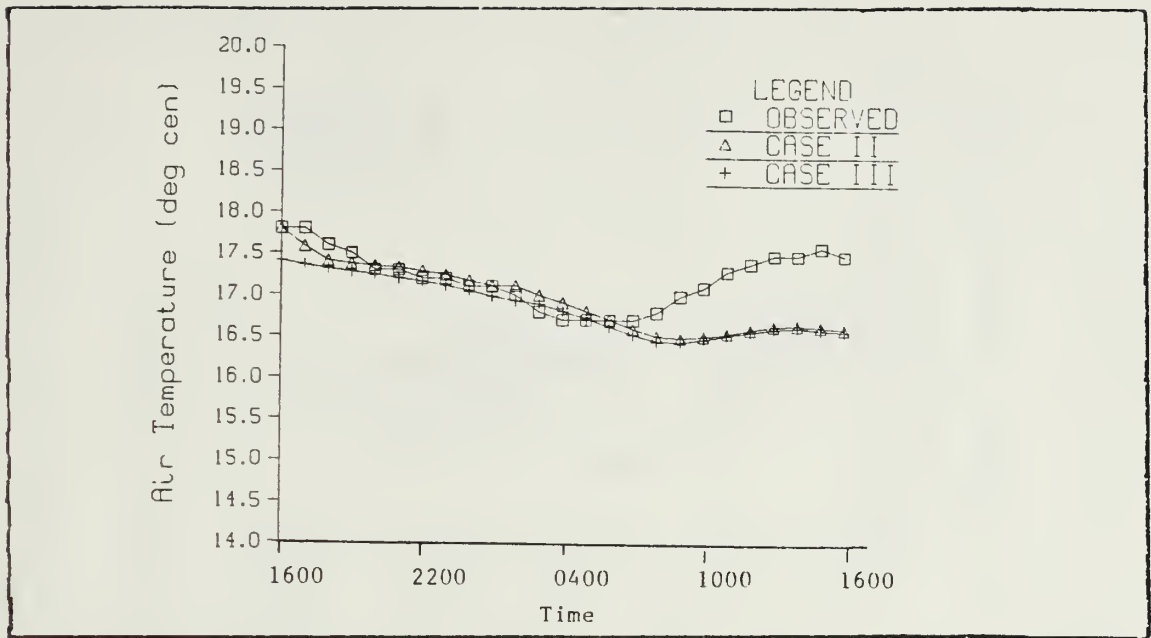
Figure 3.18    Air Temperature Comparison
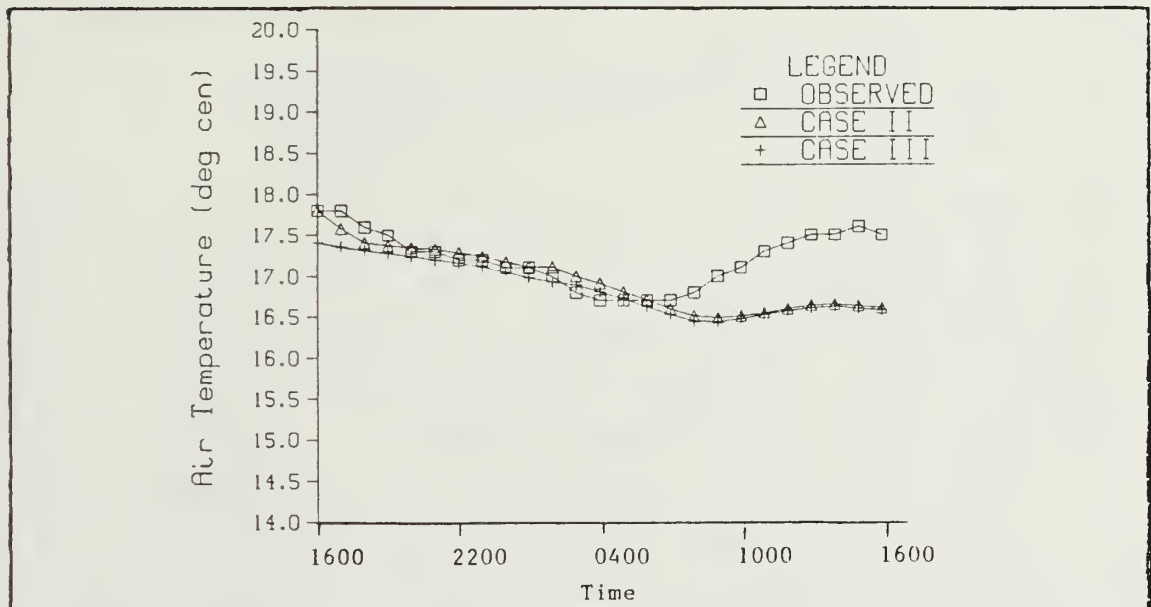Uncoupled Models



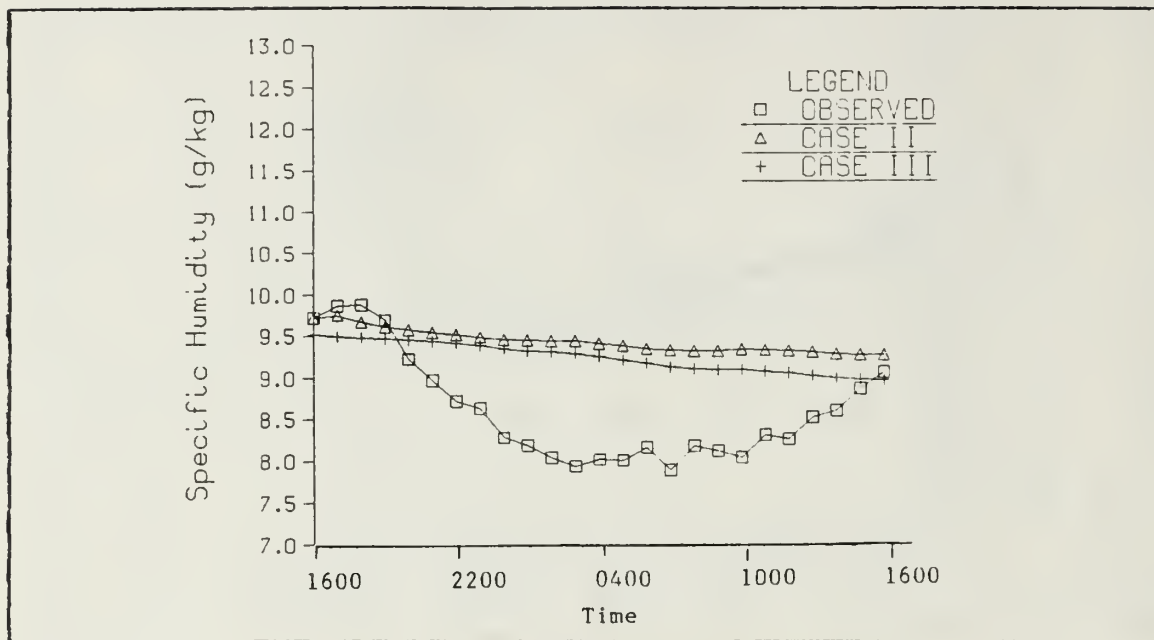Figure 3.19    Air Temperature Comparison
Coupled Models

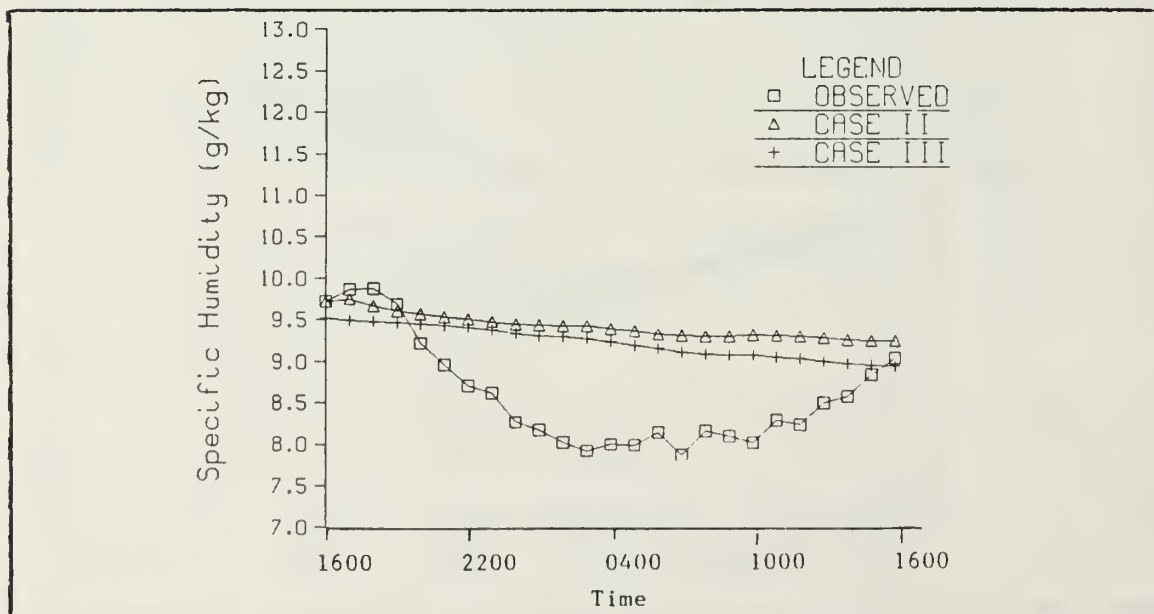Figure 3.20    Specific Humidity
Uncoupled Model



Figure 3.21    Specific Humidity
Coupled Model

54

Shortwave radiation varied as expected for the 48 hour
period, including the latter 24 hours, Figs. 3.22 and 3.23.
The order of magnitude of the difference between observed
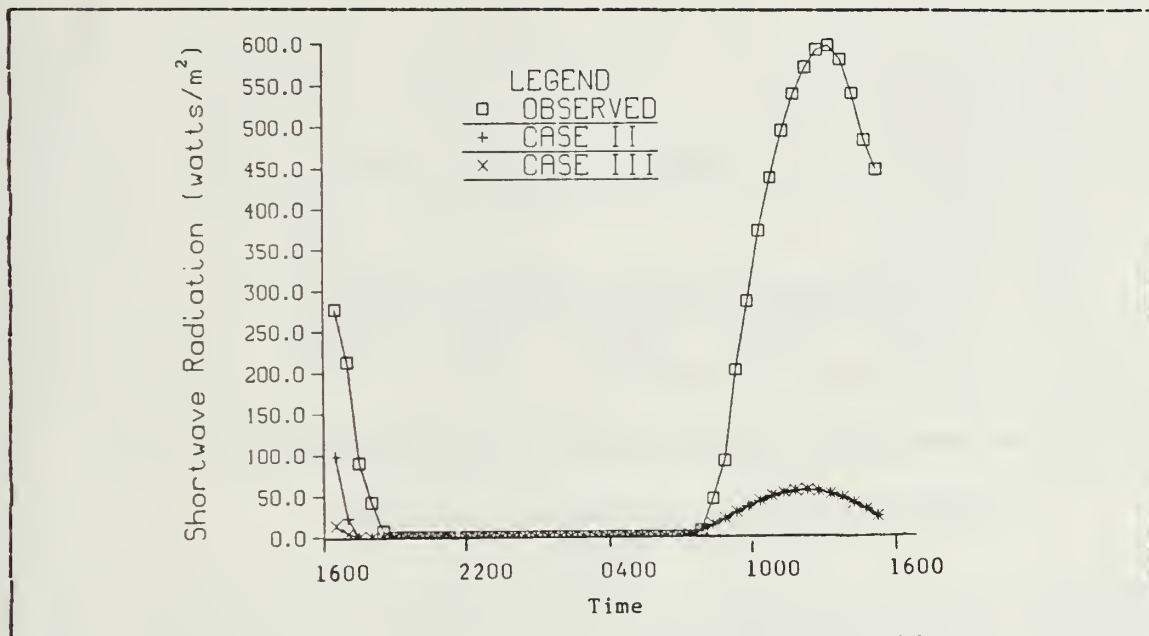and modelled values has been the same for the three cases



Figure 3.22    Shortwave Radiation
Uncoupled Model

analyzed. As in Cases I and II, the extreme cloud cover and
minimal shortwave radiation have forced significant differ-
ences in modeled variables. The impact of the predicted
radiation deficit was obvious in the behavior of air temper-
ature in Case III and was also evident in the difference
between observed and modeled mixed layer depth and sea
surface temperature.

While the mixed layer deepens in Cases II and III, the
observed mixed layer depth responds as expected to surface
heating and wind mixing, Fig. 3.24. As described in Cases I
and II, an eight hour lag exists between maximum shortwave
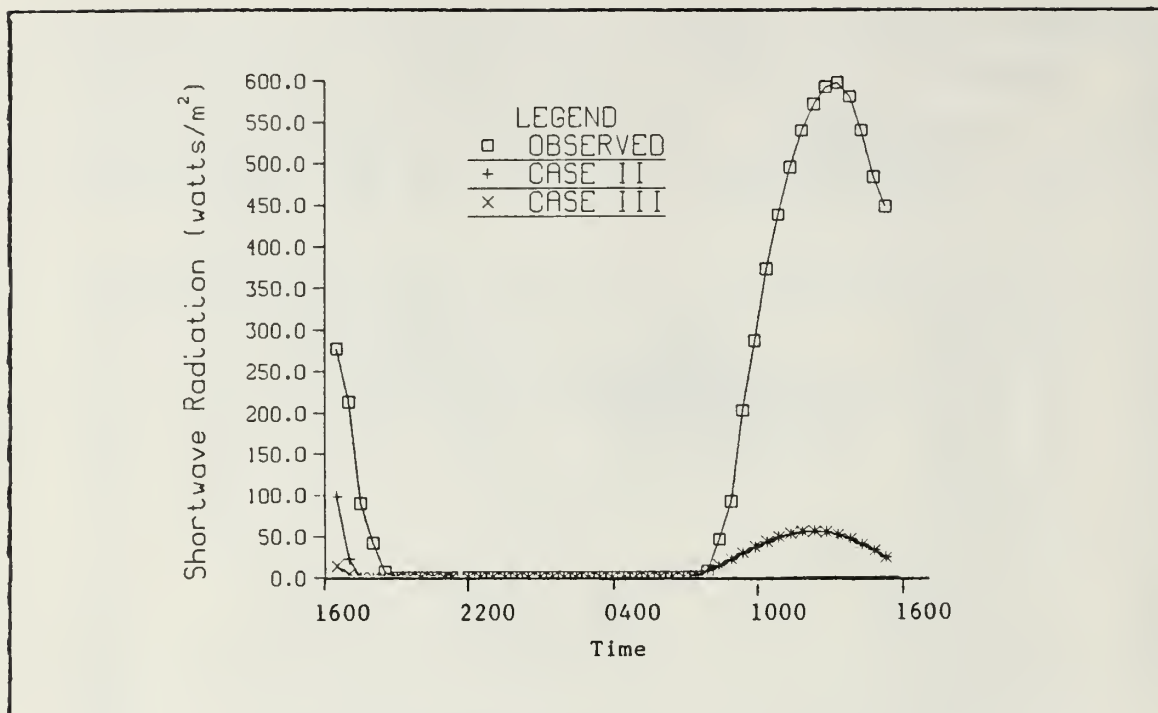radiation and maximum retreat of the mixed layer, which

55

Figure 3.23   Shortwave Radiation
Coupled Model

results from  the relatively slow  response of the  ocean to
atmospheric thermal forcing.

The modeled  cooling of the  sea surface  temperature in
all cases is  yet another effect of  the shortwave radiation
deficit, Fig. 3.25.


F.   EXPERIMENTAL SIMULATION

Based upon the results of this study,  research into the
problem of  cloud thickness prediction and  shortwave radia-
tion deficit has  begun.   Case I variables (Table I)  were
used to initialize a revised version of the model, Figs 3.26
and  3.27.   Of major  concern  is  the difference  in  the
predicted evolution of cloud  thickness.   The uncoupled and
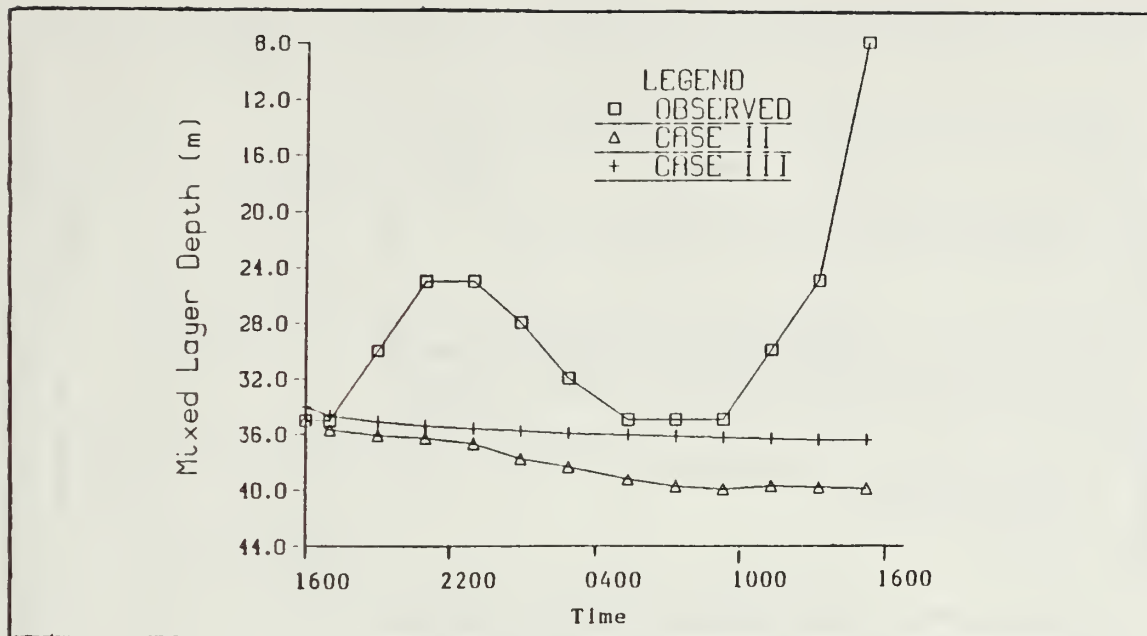coupled models predicted clouds  of thicknesses ranging from
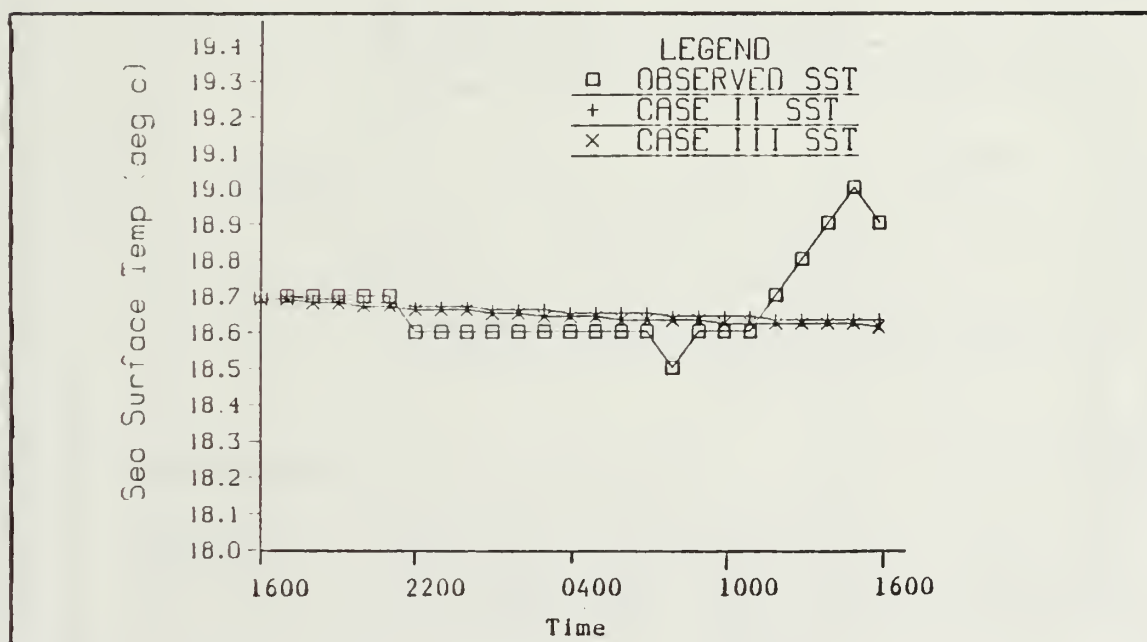
Figure 3.24    Mixed Layer Depth



Figure 3.25    Sea Surface Temperature
Coupled Model

57
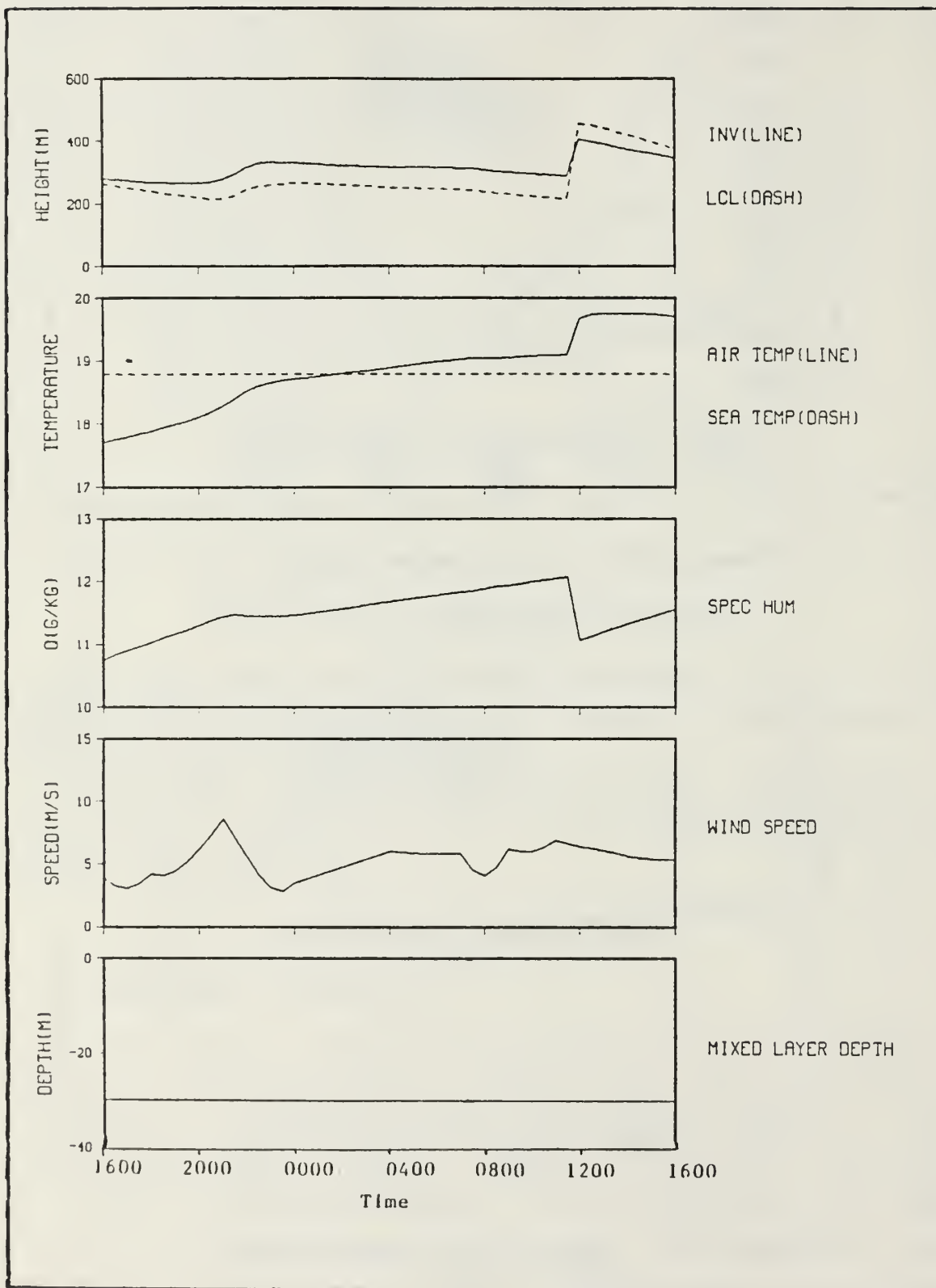
Figure 3.26    Uncoupled Model Revised

58
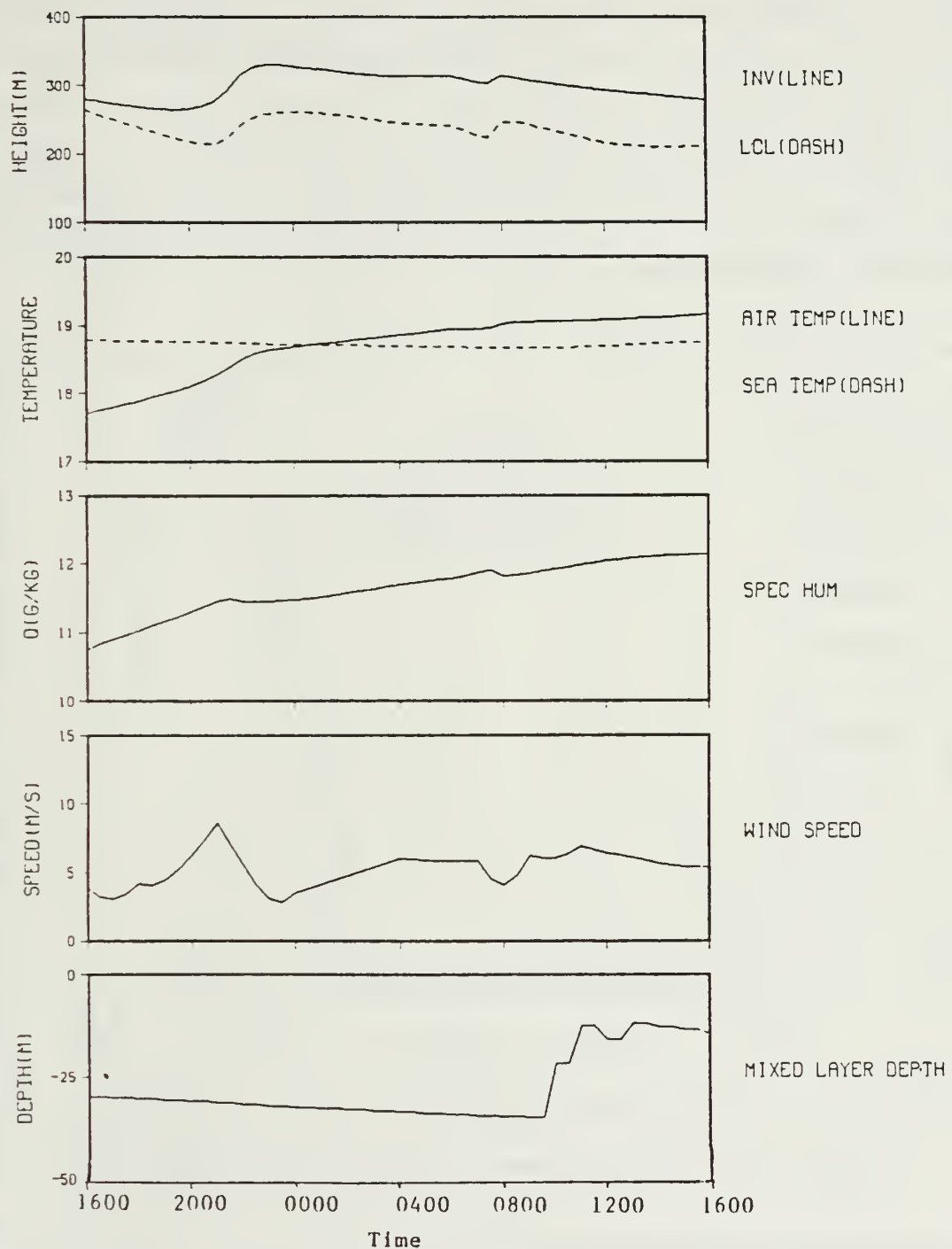
Figure 3.27    Coupled Model Revised

59

50 to 100 m. Case I clouds were originally predicted to attain a thickness of 635 m (Fig. 3.26). Predicted values of shortwave radiation are in better agreement with observations (as compared with prior cases) although differences do exist, Fig. 3.28. Mixed layer depth was predicted to shallow whereas the earlier cases demonstrated only deepening. This too was a result of the difference in the predicted evolution of shortwave radiation.
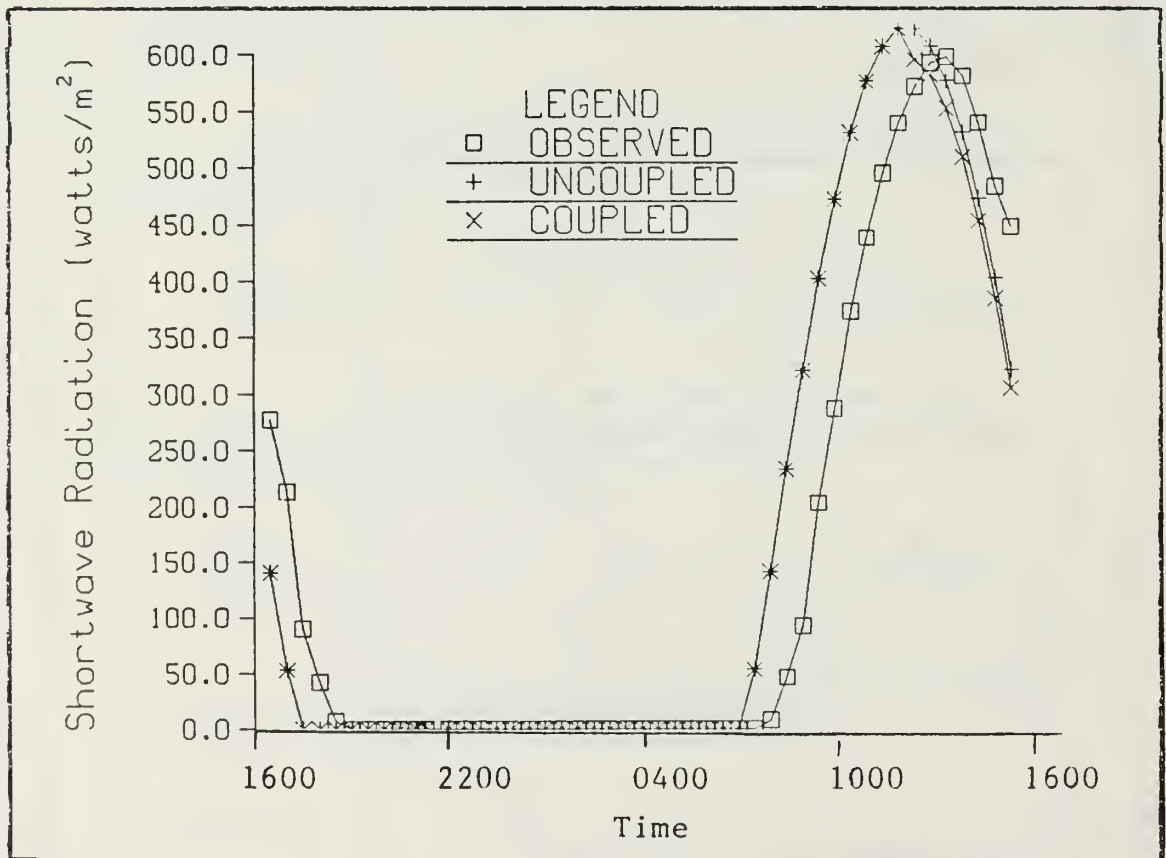


Figure 3.28    Shortwave Radiation Comparison

The evolution of predicted inversion height, LCL, air temperature and specific humidity by the uncoupled model demonstrated an extreme jump 20 hours after initialization (1200 04 Nov). As demonstrated previously, dynamic feedback

continued to occur among the predicted variables. Variations of such magnitudes however, over a period of less than 30 minutes are unrealistic.

# IV. CONCLUSIONS/RECOMMENDATIONS

Uncoupled and coupled model predictions overestimate
cloud thickness and assume an unrealistic horizon to horizon
cover. As a result, short and long wave radiative effects
are minimized. The impact of this discrepancy affects all
of the model's physics as the fluxes of heat and moisture,
variation of sea surface temperature and mixed layer depth
are improperly forced. Hence, the values for boundary layer
variables such as specific humidity, air temperature, LCL
and inversion height differ from observations.

Given this shortcoming, the model demonstrates little
variation between the coupled and uncoupled models. The
value of oceanic-atmospheric coupling has been documented
(O'Lauglin, 1982). The model behaves well for an extended
period (48 hours) when reinitialized after 24 hours.

The preliminary results obtained through the use of a
modified version of the model indicated that the model will
predict commonly observed variations in parameters such as
mixed layer depth. Similar predictions can be obtained
through the use of different experimental initializing vari-
ables. The key question which must now be investigated is
why did the original coupled and uncoupled models behave as
they did with the MILDEX observations. Due to the tentative
nature of these results, definitive conclusions concerning
the radiation and cloud modeling as it now exists cannot be
drawn. The MILDEX data set is somewhat limited in its
applicability due to gaps in the many variables required to
initialize the model. The main advantage of the data set
was the lack of platform motion during the exercise, thus
limiting advective effects which such motion may introduce.
The data set should continue to be valuable in future
studies with this model.

Cloud physics modeling must continue to be reviewed along with verification and sensitivity analyses. A multi-layer cloud model should be incorporated to examine radiation prediction. Though adequate, the slab approach currently employed is no longer essential as a means of reducing computation time. Additionally, a capability to account for partial cloudiness is absolutely essential. The total cloud cover assumption currently employed has been demonstrated by this study to be the most serious short-coming of an otherwise fundamentally sound model. A statis-tical approach in the description of cloud cover percentage is suggested as a possible solution. Further study is essential in this area.

The model should remain in a research phase of develop-ment and not be distributed for operational evaluation until the problems outlined herein are rectified. Once the model has been further refined to alleviate these problems, it should then be incorporated into a tactical environmental prediction model. Then the model will be a useful tool for the Oceanography Officer in support of fleet operations.

As for data acquisition, the performance of a navaid radiosonde system should be analyzed. The inability to record pressure and altitude for several launches severly restricted the amount of useful radiosonde data in MILDEX. Additionally, graduate student involvement in data acquisi-tion experiments is essential. Such an individual would be able to acquire a background on the data base and the atmos-pheric and oceanic situation. An exercise conducted in an area such as Monterey Bay would be useful. Such a limited body of water would further limit the advective effects of the open ocean.

63

# LIST OF REFERENCES

Araya, S.P.S., 1972: The condition for the maintenance of turbulence in stratified flows. Quart. J. Roy. Meteor. Soc., 98, 264-273.

Businger, J.A., 1973: Turbulent transfer in the atmospheric surface layer. Workshop on Micrometeorology, D.A. Haugen, Ed., Amer. Meteor. Soc., 392 pp.

Davidson, K.L., C.W. Fairall, P.J. Boyle, and G.E. Schacher, 1984: Verification of an atmospheric mixed-layer model for a coastal region. J. Climate Appl. Meteor., 617-636.

Fleagle, R.G., and J.A. Businger, 1980: An Introduction to Atmospheric Physics. 2nd ed. Academic Press, 432 pp.

Garwood, R.W. Jr., 1977: An ocean mixed layer model capable of simulating cyclic states. J. Phys. Oceanogr., 7, 455-468.

Geerneart, G.L., P.S. Guest, C.E. Skupniewicz, D.E. Spiel, K.L. Davidson, W.J. Shaw, K.B. Katsaros, and R.J. Lind, 1984: Meteorology report for the 1983 Mixed Layer Dynamics Experiment (MILDEX). Tech. Rep. NPS-63-84-002, Naval Postgraduate School, Monterey, Ca., 128 pp.

Gleason, J.P., 1982: Single station assessments of the synoptic scale forcing on the marine atmospheric boundary layer. M.S. Thesis, Naval Postgraduate School, Monterey, Ca., 55 pp.

Hervey, R.V., 1983: Sensitivity analys of a coupled atmospheric-oceanic boundary layer model. M.S. Thesis, Naval Postgraduate School, Monterey, Ca, 61 pp.

Husby, D.M., and G.R. Seckel, 1978: Large scale air-sea interactions at ocean station V. NOAA Tech. Rep. NMFS SSRF-696, 44 pp.

Joseph, J.H., W.J. Wiscomb, and J.A. Weinman, 1976: The delta-Eddington approximation for radiative flux transfer. J. Atmos. Sci., 33, 2452-2459.

Miller, J.R., 1976: The salinity effects in a mixed layer ocean model. J. Phys. Oceanogr., 6, 29-35.

O'Laughlin, M.C., 1982: Formulation of a prototype
    atmospheric and oceanic boundary layer model. M.S.
    Thesis, Naval Postgraduate School, Monterey, Ca., 89 pp.

Slingo, A.S., S. Nicholls, and C.L. Wrench, 1982: A field
    study of nocturnal stratocumulus: III, High rsolution
    radiative and microphysical observations.  Quart. J. Roy.
    Meteor. Soc., 108, 145-166.

Staje, S.A., and J.A. Businger, 1981: A model for
    entrainment into a cloud topped marine boundary layer-
    part I: model description and application to a cold air
    outbreak episode.  J. Atmos. Sci., 38, 2213-2229.

Tennekes, H. and A.G.M. Dreidonks, 1981: Basic entrainment
    equations for the atmospheric boundary layer.  Bound.
    Layer Meteor., 20, 515-531.

# INITIAL DISTRIBUTION LIST

|  |  | No. Copies |
|---|---|---|
| 1. | Defense Technical Information Center<br>Cameron Station<br>Alexandria ,VA 22314 | 2 |
| 2. | Library, Code 0142<br>Naval Postgraduate School<br>Monterey, CA 93943 | 2 |
| 3. | Professor C.N.K. Mooers, Code 68Mr<br>Naval Postgraduate School<br>Monterey, CA 93943 | 1 |
| 4. | Professor R.J. Renard, Code 63Rd<br>Naval Postgraduate School<br>Monterey, CA 93943 | 1 |
| 5. | Professor R.W. Garwood, Code 68 Gd<br>Naval Postgraduate School<br>Monterey, CA 93943 | 3 |
| 6. | Professor K.L. Davidson, Code 63Ds<br>Naval Postgraduate School<br>Monterey, CA 93943 | 3 |
| 7. | Professor C.R. Dunlap, Code 68Du<br>Naval Postgraduate School<br>Monterey, CA 93943 | 1 |
| 8. | Director<br>Naval Oceanography Division<br>Naval Observatory<br>34TH and Massachusetts Ave. NW<br>Washington, D.C. 20390 | 1 |
| 9. | Commander<br>Naval Oceanography Command<br>NSTL Station<br>Bay St. Louis, MS 39522 | 1 |
| 10. | Commanding Officer<br>ATTN: LCDR John Burger<br>Naval Oceanography Office<br>NSTL Station<br>Bay ST. Louis, MS 39522 | 1 |
| 11. | Commanding Officer<br>Fleet Numerical Oceanography Center<br>Monterey, CA 93940 | 1 |
| 12. | Commanding Officer<br>Naval Ocean Research and Development Activity<br>NSTL Station<br>Bay St. Louis, MS 39522 | 1 |
| 13. | Commanding Officer<br>Naval Environmental Prediction Research Facility<br>Monterey, CA 93940 | 1 |

14. Chairman Oceanography Department                           1
    U.S. Naval Academy
    Annapolis, MD 21402

15. Chief of Naval Research                                     1
    800 N. Quincy Street
    Arlington, VA 22217

16. Office of Naval Research (Code 422)                         1
    Naval Oceanography Research and Development
    Activity
    NSTL Station
    Bay St. Louis, MS 39522

17. Scientific Liaison Office                                   1
    Office of Naval Research
    Scripts Institute of Oceanography
    La Jolla, CA 92037

18. Library                                                     1
    Scripps Institute of Oceanography
    P.O. Box 2367
    La Jolla, CA 92307

19. Commander                                                   1
    Oceanographic Systems Pacific
    Box 1390
    Pearl Harbor, HI 96860

20. LCDR Joseph W. Swaykos                                      2
    Naval Oceanography Command Detachment
    Box 57, Naval Air Station
    Brunswick, ME 04011

22. Commanding Officer                                          1
    Naval Oceanography Command Facility
    NAS North Island
    San Diego, CA 92135

23. Dr. T. Spence (Code 422PO)                                  1
    Office of Naval Research
    800 North Quincy St.
    Arlington, VA 22217

24. Dr. Paul Twitchell (Code 331C)                             1
    Naval Air Systems Command
    Washington, D.C. 20360

213139

Thesis
S9269      Swaykos
c.1           Simulation of the
           coupled atmospheric
           and oceanic boundary
           layer model during
           MILDEX.